

**Research Activities
in
NTT Basic Research Laboratories**

**Volume 19
Fiscal 2008**

July 2009

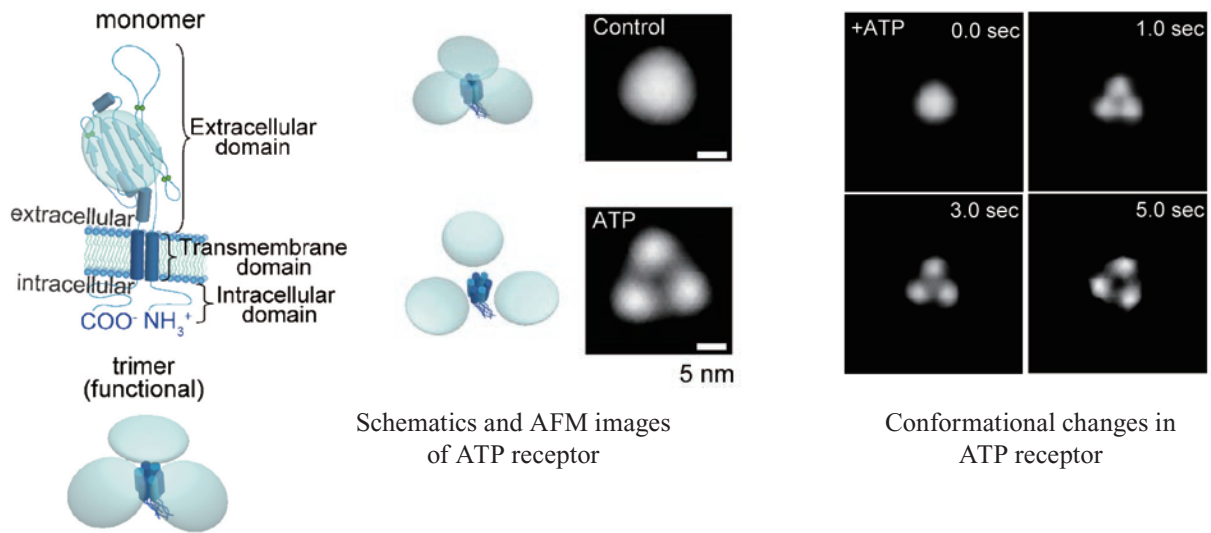
**NTT Basic Research Laboratories,
Nippon Telegraph and Telephone Corporation (NTT)**

<http://www.brl.ntt.co.jp/>

Cover photograph:

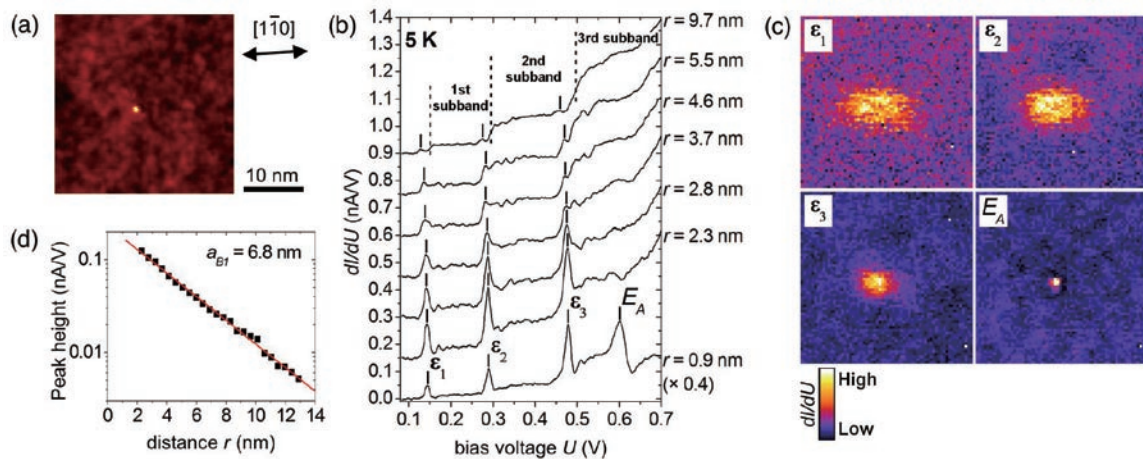
Self-Assembled Gold Nanorod Arrays

Designed array structures of gold nanorods (diameter: 10 nm, length: 40 nm). The surface of gold nanorod is modified by lipid molecules or polymers etc. A variety of building blocks of gold nanorods are successfully fabricated via self-assembly of the surface anchored molecules. The gold nanorod arrays are applicable for nano plasmonic materials or highly sensitive biochips that can detect intermolecular interactions on a single molecular scale.



Observation of Ligand-Induced Conformational Changes in Single ATP Receptors with Fast-Scanning Atomic Force Microscopy

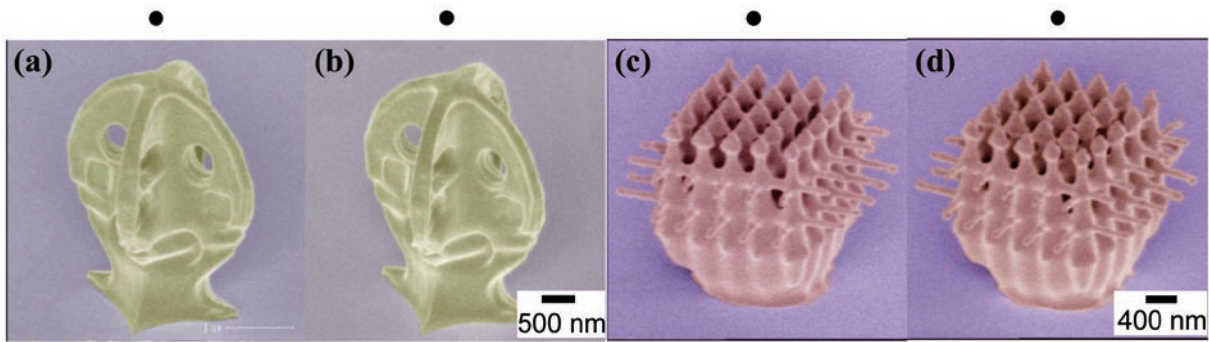
Proteins, known as "receptors" that exist in cells, exhibit their functions via binding with small compounds such as hormones. When the receptor is a type of ion channel, it opens its pore after binding with compounds thereby flowing ions through it and resulting in exhibiting its function. We observed the topology and stimulation-induced conformational changes in adenosine triphosphate (ATP) receptor, an important receptor in pain sensation, with atomic force microscopy (AFM). (Page 20)



(a) STM topography of a single donor (bright spot). (b) Distance r dependence of LDOS from a single donor. Energy positions $\epsilon_1 \sim \epsilon_3$ give bound state levels. (c) Spatial LDOS maps at $\epsilon_1 \sim \epsilon_3$. (d) LDOS intensity of the lowest energy level ϵ_1 as a function of distance r . By measuring this dependence, the Bohr radius (a_{BI}) is determined.

Direct Measurement of the Binding Energy and Bohr Radius of a Single Hydrogenic Defect in a Semiconductor Quantum Well

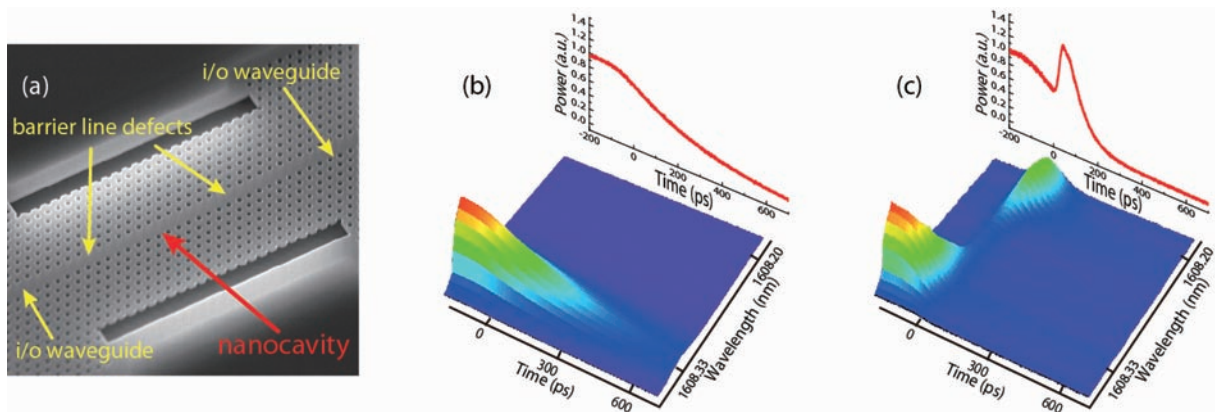
It is well known that the behavior of donor impurities, which are very important for semiconductor devices, can be approximately understood by the hydrogenic model. The two fundamental properties are the binding energy and the Bohr radius. However, These values have not been characterized for a single donor before. By measuring the local density of states (LDOS) in the vicinity of the defect at the semiconductor quantum well surface using low-temperature scanning tunneling microscopy (STM), we have succeeded in determining both the binding energy and the Bohr radius. (Page 28)



3D nanostructure in positive resist [(a), (b)] and another structure in negative resist [(c), (d)]. As each pair constitutes a stereogram, 3D images can be seen with parallel viewing.

Fabrication of Three-Dimensional Nanostructures by Electron Beam Lithography

New methods in three-dimensional nanofabrication technique using electron beam (EB) lithography have been devised, promising nanotechnology applications. The accuracy of 3D positioning (i.e., 3D alignment) has been improved up to the order of 10 nm. Moreover, effective suppression of the proximity effect due to electron scattering has been achieved, enabling us to freely fabricate various 3D nanostructures. (Page 27)



(a) Scanning electron microscope image of a fabricated width-modulated line-defect photonic crystal nanocavity. The air holes in the nanocavity are shifted slightly outside the line defect. The 3D plots shown in (b) and (c) are measured spectrograms of the output light at a waveguide after it had been trapped in the photonic crystal nanocavity. The graphs behind the 3D plots are spectrally convoluted temporal waveforms. (b) Output without modulation. (c) Output when the cavity is modulated at $t=0$ ps. The wavelength of the trapped light shifts towards a shorter wavelength as a result of adiabatic wavelength conversion, and the light is immediately output into the waveguides and generates a short pulse.

Short Pulse Generation by Adiabatic Wavelength Shifting

Photonic crystal nanocavities have a long photon lifetime, which enables us to manipulate photons while they are trapped. For example, we can adiabatically change the wavelength of the trapped light by changing the refractive index of the cavity, which is analogous to a vibrating string of a guitar. As a result of the adiabatic wavelength shifting of light, we can demonstrate the Q switching of a very small cavity integrated on a silicon chip. We demonstrate short pulse generation from a very high Q cavity with arbitrary timing by adiabatic wavelength shifting. This demonstration paves the way to the development of an on-chip photon memory. (Page 41)

Message from the Director



We are deeply grateful for your interest and support with respect to our research activities.

Our mission is to overcome technological obstacles such as providing high-capacity transmission and delivering absolutely safe telecommunication. To achieve these goals, we are focusing on 1. Iconoclastic Science and Technology, 2. Innovative technologies, 3. Incubating new ideas and strengthening our competences. This will allow us to contribute to the success of NTT's business and promote advances in science that we hope will ultimately benefit all mankind.

As we proceed with our research, there are some very high barriers to overcome and we are also facing the demand to make speedy progress. If we are to achieve our goals, it is important that we adopt a global perspective in relation to our research activities, and to this end we are actively collaborating with many universities and research institutes throughout the world as well as with other NTT laboratories. To help promote a public understanding of our activities and frank exchanges of opinion, BRL holds a "Science Plaza" every year. We also host international conferences at NTT Atsugi R&D Center. The International Symposium on Nanoscale Transport and Technology (ISNTT2009) was held in January 2009, and more than 200 people attended. Moreover, one of our missions is the education of young researchers and we have sponsored four "BRL Schools" since 2002. The BRL School boasts distinguished researchers as lecturers, and on each occasion more than 30 graduate students from both at home and abroad have felt its benefit. We hope that this endeavor will encourage research and contribute to its future growth.

It gives us immense pleasure to fulfill our mission of being an open laboratory in this way, and to disseminate our research output worldwide. Your continued support is greatly appreciated.

A handwritten signature in black ink, which reads "Junji Yumoto". The signature is fluid and cursive, with the first name "Junji" and the last name "Yumoto" clearly distinguishable.

Junji Yumoto
Director
NTT Basic Research Laboratories

Contents

	page
◆ Color Frontispiece	I
◆ Observation of Ligand-Induced Conformational Changes in Single ATP Receptors with Fast-Scanning Atomic Force Microscopy	
◆ Direct Measurement of the Binding Energy and Bohr Radius of a Single Hydrogenic Defect in a Semiconductor Quantum Well	
◆ Fabrication of Three-Dimensional Nanostructures by Electron Beam Lithography	
◆ Short Pulse Generation by Adiabatic Wavelength Shifting	
◆ Message from the Director	III
◆ Member List	1
I. Research Topics	
◇ Overview of Research in Laboratories	11
◇ Materials Science Laboratory	12
◆ Boron-Implanted Diamond FETs Formed by Ion-Implantation and High-Pressure and High-Temperature Annealing	
◆ High Performance Nitride-Based Heterojunction Bipolar Transistors on GaN Substrates	
◆ Anisotropic In-Plane Strains in Non-Polar $\text{Al}_{1-x}\text{Ga}_x\text{N}$ ($1\bar{1}20$) Films ($x < 0.2$)	
◆ Molecular Beam Epitaxial Growth of Hexagonal Boron Nitride on Ni(111) Substrate	
◆ Simultaneous Optical and Electrical Characterization at Nanoscale with Scanning Probe Microscope	
◆ Diameter Dependence of Hydrogen Adsorption on Single-Walled Carbon Nanotubes	
◆ Number-of-Layers Dependence of Electronic Properties of Epitaxial Few-Layer Graphene	
◆ Precise Control of Gold Nanorod Arrays	
◆ Observation of Ligand-Induced Conformational Changes in Single ATP Receptors with Fast-Scanning Atomic Force Microscopy	
◆ The Preferential Reconstitution of Receptor Proteins into Model Lipid Domains Studied by Atomic Force Microscopy	
◆ Effect of Nanogap on Dynamics of Lipid Bilayer	
◇ Physical Science Laboratory	23
◆ Stochastic Data Processing Based on Single Electrons Using Nano Field-Effect Transistors	
◆ Identification of Single Dopant Position in Silicon Nanotransistor	
◆ Bit Operation in a Parametrically Pumped Electromechanical Resonator	
◆ In-plane Conductance Measurements of Few-Layer Graphene on SiC Substrate	

◆ Fabrication of Three-Dimensional Nanostructures by Electron Beam Lithography	
◆ Direct Measurement of the Binding Energy and Bohr Radius of a Single Hydrogenic Defect in a Semiconductor Quantum Well	
◆ Electrons and Holes in a Single Silicon Slab	
◆ New Readout Method for Josephson Persistent-Current Qubits Using a Josephson Bifurcation Amplifier	
◆ Evidence of Noise-Suppression with Superconductive Atom Chip	
◆ Single-Shot Readout of a Josephson Persistent Current Quantum Bit	
◆ Photoluminescence Spectroscopy of Nonlinear- and Linear-Screening Regimes in a Low-Density Two-Dimensional Electron System	
◆ Negative Photoconductivity in $\text{In}_{0.52}\text{Al}_{0.48}\text{As}/\text{In}_{0.7}\text{Ga}_{0.3}\text{As}$ Heterostructures	
◇ Optical Science Laboratory	35
◆ Numerical Simulation of Ultracold Atoms Trapped in Optical Lattices	
◆ Single Photon Detection Using MgB_2 Superconductor	
◆ Generation of High-Purity Entangled Photon Pairs Using Silicon Wire Waveguide	
◆ Efficient Carrier Envelope Offset Locking for a Frequency Comb by Modifying a Collinear f -to- $2f$ Interferometer	
◆ Cavity Emission and Photon Statistics in Exciton-Cavity Coupled Systems	
◆ Magneto-Optical Spectroscopy of Charge-Tunable Quantum Dots	
◆ Short Pulse Generation by Adiabatic Wavelength Shifting	
◆ Ultrahigh- Q Photonic Crystal Slab Nanocavities in Very Thin Barriers	
◆ Dynamic High- Q Cavity Formation and Photon Pinning by Index Modulation	

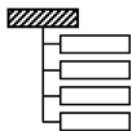
II. Data

◇ Science Plaza 2008	45
◇ ISNTT2009	46
◇ The 5th Advisory Board	47
◇ Award Winners' List	48
◇ In-house Award Winners' List	49
◇ List of Visitors' Talks	50
◇ Research Activities in Basic Research Laboratories in 2008	54
◇ List of Invited Talks at International Conferences	56

Member List

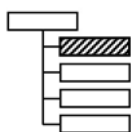
As of March 31, 2009
(* moved to another position within a year)

NTT Basic Research Laboratories



Director, **Dr. Junji Yumoto**

Research Planning Section



Executive Research Scientist,

Dr. Toshiki Makimoto

Senior Research Scientist,

Dr. Kazuhide Kumakura
Dr. Hideki Gotoh*

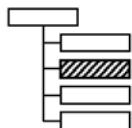
Senior Research Scientist,

Dr. Kazuaki Furukawa
Dr. Koji Muraki*

NTT Research Professor

Dr. Fujio Shimizu
(The University of Electro-Communications)
Prof. Shintaro Nomura
(University of Tsukuba)
Prof. Kyo Inoue
(Osaka University)
Dr. Yukihiro Tamba
(Shizuoka University)

Materials Science Laboratory



Executive Manager, **Dr. Keiichi Torimitsu**

Assistant Manager, Dr. Satoru Suzuki
Dr. Hiroo Omi*

Thin-Film Materials Research Group:

Dr. Makoto Kasu (Group Leader)

Dr. Yasuyuki Kobayashi	Dr. Hideki Yamamoto	Dr. Hisashi Sato
Dr. Tetsuya Akasaka	Dr. Kazuhide Kumakura*	Dr. Yoshitaka Taniyasu
Dr. Kenji Ueda	Dr. Atsushi Nishikawa*	Dr. Chiun-Lung Tsai
Dr. Michal Kubovic		

Low-Dimensional Nanomaterials Research Group:

Dr. Yoshihiro Kobayashi (Group Leader)

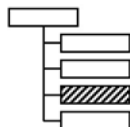
Dr. Fumihiko Maeda	Dr. Hiroki Hibino	Dr. Hiroo Omi
Dr. Satoru Suzuki*	Akio Tokura	Dr. Ilya Sychukov
Dr. Daisuke Takagi		

Molecular and Bio Science Research Group:

Dr. Keiichi Torimitsu (Group Leader)

Dr. Keisuke Ebata	Dr. Kazuaki Furukawa*	Dr. Koji Sumitomo
Dr. Nahoko Kasai	Dr. Akiyoshi Shimada	Dr. Hiroshi Nakashima
Dr. Yoshiaki Kashimura	Toichiro Goto	Dr. Youichi Shinozaki

Physical Science Laboratory



Executive Manager, **Dr. Hiroshi Yamaguchi**

Assistant Manager, Dr. Kenji Yamazaki
Dr. Yukinori Ono*
Takeshi Karasawa

Nanodevices Research Group:

Dr. Akira Fujiwara (Group Leader)

Dr. Yukinori Ono Dr. Hiroyuki Kageshima Dr. Katsuhiko Nishiguchi
Dr. Jin-ichiro Noborisaka Dr. Mohammed A. H. Khalafalla

Nanostructure Technology Research Group:

Dr. Hiroshi Yamaguchi (Group Leader)

Dr. Masao Nagase Dr. Kenji Yamazaki* Toru Yamaguchi
Dr. Hajime Okamoto Dr. Koji Onomitsu Dr. Imran Mahboob
Dr. Vijay Singh

Quantum Solid State Physics Research Group:

Dr. Koji Muraki (Group Leader)

Dr. Toshimasa Fujisawa*

Dr. Kiyoshi Kanisawa Dr. Satoshi Sasaki* Dr. Kyoichi Suzuki
Dr. Toshiaki Hayashi Dr. Takeshi Ota Dr. Norio Kumada
Dr. Kei Takashina Dr. Kasper Grove-Rasmussen
Dr. Gerardo Gamez

Superconducting Quantum Physics Research Group:

Dr. Kouichi Semba (Group Leader)

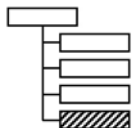
Dr. Hayato Nakano Dr. Tetsuya Mukai Dr. Shiro Saito
Dr. Shin-ichi Karimoto Hirotaka Tanaka Dr. Kousuke Kakuyanagi
Dr. Ying-Dan Wang* Dr. Yoshiharu Yamada Dr. Hideyuki Sawamura
Dr. Alexandre Kemp Dr. Xiaobo Zhu

Spintronics Research Group:

Dr. Tatsushi Akazaki (Group Leader)

Dr. Yuichi Harada Dr. Hiroyuki Tamura Dr. Masumi Yamaguchi
Dr. Yoshiaki Sekine

Optical Science Laboratory



Executive Manager, **Dr. Yasuhiro Tokura**

Assistant Manager, Dr. Satoshi Sasaki
Dr. Atsushi Yokoo*

Quantum Optical State Control Research Group:

Dr. Yasuhiro Tokura (Group Leader)

Dr. Kaoru Shimizu

Dr. Makoto Yamashita

Dr. Fumiaki Morikoshi

Daisuke Hashimoto

Kazuhiro Igeta

Dr. Hiroyuki Shibata

Dr. Toshimori Honjo

Dr. Ken-ichi Harada

Masami Kumagai

Dr. Hiroki Takesue

Dr. Kiyoshi Tamaki

Quantum Optical Physics Research Group:

Dr. Hidetoshi Nakano (Group Leader)

Dr. Tadashi Nishikawa

Dr. Kouta Tateno

Dr. Atsushi Ishizawa

Dr. Keiko Kato

Dr. Hideki Gotoh

Dr. Takehiko Tawara

Dr. Haruki Sanada

Hidehiko Kamada

Dr. Katsuya Oguri

Dr. Guoqiang Zhang

Photonic Nano-Structure Research Group:

Dr. Masaya Notomi (Group Leader)

Dr. Satoki Kawanishi

Dr. Akihiko Shinya

Dr. Hisashi Sumikura

Dr. Atsushi Yokoo

Dr. Hideaki Taniyama

Dr. Kengo Nozaki

Dr. Eiichi Kuramochi

Dr. Takasumi Tanabe

Dr. Young-Geun Roh

Distinguished Technical Members



Masaya Notomi was born in Kumamoto, Japan on February 16, 1964. He received his B.E., M.E. and Dr. Eng. degrees in applied physics from The University of Tokyo, Japan in 1986, 1988, and 1997, respectively. In 1988, he joined NTT Optoelectronics Laboratories. Since then, his research interest has been to control the optical properties of materials and devices by using artificial nanostructures, and engaged in research on semiconductor quantum wires/dots and photonic crystal structures. He has been in NTT Basic Research Laboratories since 1999, and is currently working on light-propagation control by use of various types of photonic crystals. From 1996-1997, he was with Linköping University in Sweden as a visiting researcher. He is also a guest associate professor of Tokyo Institute of Technology (2003-). He received IEEE/LEOS Distinguished Lecturer Award in 2006, JSPS (Japan Society for the Promotion of Science) prize in 2009, and Japan Academy Medal in 2009. He is a member of the Japan Society of Applied Physics, APS, IEEE/LEOS, and OSA.



Akira Fujiwara was born in Tokyo, Japan on March 9, 1967. He received his B.S., M.S., and Ph.D. degrees in applied physics from The University of Tokyo, Japan in 1989, 1991, and 1994, respectively. In 1994, he joined NTT LSI Laboratories and moved to NTT Basic Research Laboratories in 1996. Since 1994, he has been engaged in research on silicon nanostructures and their application to single-electron devices. He was a guest researcher at the National Institute of Standards and Technology (NIST), Gaithersburg, MD, USA during 2003-2004. He received the SSDM Young Researcher Award in 1998, SSDM Paper Award in 1999, and Japanese Journal of Applied Physics (JJAP) Paper Awards in 2003 and 2006. He was awarded the Young Scientist Award from the Minister of MEXT (Ministry of Education, Culture, Sports, Science, and Technology) in 2006. He is a member of the Japan Society of Applied Physics and IEEE.

Advisory Board (2008 Fiscal Year)

Name	Affiliation
Prof. Gerhard Abstreiter	Walter Schottky Institute, Germany
Prof. Boris L. Altshuler	Department of Physics, Columbia University, U.S.A.
Prof. Serge Haroche	Département de Physique, École Normale Supérieure, France
Prof. Mats Jonson	Department of Physics, Göteborg University, Sweden
Prof. Anthony J. Leggett	Department of Physics, University of Illinois at Urbana-Champaign, U.S.A.
Prof. Johan E. Mooij	Kavli Institute of Nanoscience, Delft University of Technology, the Netherlands
Prof. John F. Ryan	Clarendon Laboratory, University of Oxford, U.K.
Prof. Klaus von Klitzing	Max-Planck-Institut für Festkörperforschung, Germany
Prof. Theodor W. Hänsch	Max-Planck-Institut für Quantenoptik, Germany

Invited / Guest Scientists (2008 Fiscal Year)

Name	Affiliation	Period
Dr. Go Yusa	Japan Science and Technology Agency (JST), Japan	Apr. 2008 – Mar. 2009
Assoc. Prof. Takaaki Koga	Hokkaido University, Japan	Apr. 2008 – Mar. 2009
Dr. Keiko Kato	National Institute for Materials Science (NIMS), Japan	Apr. 2008 – Jun. 2008
Dr. Hideomi Hashiba	Institute of Quantum Science, Nihon University, Japan	Apr. 2008 – Mar. 2009
Dr. Shoko Utsunomiya	National Institute of Informatics, Japan	Apr. 2008 – Mar. 2009
Dr. Takashi Uchida	Toyo University (School of Engineering), Japan	May 2008 – Mar. 2009
Dr. Chandra Ramanujan	University of Oxford, U.K.	Nov. 2008 – Dec. 2008
Dr. Nicolas Clement	Institut of Electronics, Microelectronics and Nanotechnology (IEMN), France	April 2008
Prof. Stephen Hughes	Department of Physics, Queen's University, Canada	Sep. 2008 – Oct. 2008
Prof. Amnon Aharony	Ben-Gurion University of the Negev, Israel	October 2008
Prof. Ora Entin-Wohlman	Ben-Gurion University of the Negev, Israel	October 2008
Prof. Christos Flytzanis	École Normale Supérieure (ENS), France	Nov. 2008 – Dec. 2008
Prof. Jocelyn Achard	University of Paris XIII, France	Dec. 2008 – Jan. 2009

Overseas Trainees (2008 Fiscal Year)

Name	Affiliation	Period
Christoph Hufnagel	University of Heidelberg, Germany	Jun. 2006 –
Yosia	Nanyang Technological University, Singapore	Apr. 2007 – Apr. 2008
Edita Kirpsaite	Kaunas University of Technology, Lithuania	Jan. 2008 – Aug. 2008
John McGurk	Imperial College London, U.K.	Jan. 2008 – Aug. 2008
Miron Sadziak	Warsaw University, Poland	Jan. 2008 – Aug. 2008
Zhenzhong Wang	Chinese Academy of Sciences, China.	Jan. 2008 – Dec. 2008
Thibaut Balois	École Normale Supérieure, France	Feb. 2008 – Jul. 2008
Thomas Panier	École Normale Supérieure, France	Feb. 2008 – Jul. 2008
Benjamin Miquel	École Normale Supérieure, France	Feb. 2008 – Jul. 2008
Samir Etaki	Delft University of Technology, the Netherlands	May 2008 – Dec. 2008
Taige Hou	MIT (Massachusetts Institute of Technology), U.S.A.	May 2008 – Aug. 2008
Jaap Kautz	University of Twente, the Netherlands	May 2008 – Aug. 2008
Christopher Jackson	University of Nottingham, U.K. .	Jun. 2008 – Aug. 2008
Aurelien Peilloux	ESPCI (École Supérieure de Physique et de Chimie Industrielle), France	Jul. 2008 – Dec. 2008
Charline Froitier	ESPCI (École Supérieure de Physique et de Chimie Industrielle), France	Jul. 2008 – Dec. 2008
Paul Boniface	ESPCI (École Supérieure de Physique et de Chimie Industrielle), France	Jul. 2008 – Dec. 2008
Thomas Keen	University of Oxford, U.K. .	Aug. 2008 – Aug. 2008
Ferry Prins	Delft University of Technology, the Netherlands	Sep. 2008 – Oct. 2008
Jelena Baranovic	University of Oxford, U.K.	Sep. 2008 – Oct. 2008
Maarten Nijland	University of Twente, the Netherlands	Jan. 2009 – Apr. 2009
Stefano Salvatore	Technical University, Milan, Italy	Sep. 2008 – Oct. 2008
Corentin Durand	University of Lille/ ISEN-Lille, France	Feb. 2009 – Jul. 2009
Pauline Renoux	INSA (Institut National des Sciences Appliquées de Toulouse), France	Feb. 2009 –
Laurent-Daniel Haret	Institut d' Optique Graduate School, France	Feb. 2009 –

Domestic Trainees (2008 Fiscal Year)

Name	Affiliation	Period
Mizuki Miyamoto	Shonan Institute of Technology, Japan	Apr.2008 – Mar.2009
Hiroshi Sakai	Tokyo University of Science, Japan	Apr.2008 – Mar.2009
Kenji Yamaya	Tokyo University of Science, Japan	Apr.2008 – Mar.2009
Norihito Hibino	Keio University, Japan	Apr.2008 – Mar.2009
Hiroyuki Wakahara	Keio University, Japan	Apr.2008 – Mar.2009
Akira Wada	Tohoku University, Japan	Apr.2008 – Mar.2009
Satoru Miyamoto	Keio University, Japan	Apr.2008 – Mar.2009
Yasuaki Miyazaki	Keio University, Japan	Apr.2008 – Mar.2009
Kuniaki Yamada	Keio University, Japan	Apr.2008 – Mar.2009
Keiichiro Nonaka	The University of Tokyo, Japan	Apr.2008 – Mar.2009
Kojiro Tamaru	The University of Tokyo, Japan	Apr.2008 – Mar.2009
Takehito Kamata	Tohoku University, Japan	Apr.2008 – Mar.2009
Kenichi Hitachi	The University of Tokyo, Japan	Apr.2008 – Mar.2009
Gou Shinkai	Tokyo Institute of Technology, Japan	Apr.2008 – Mar.2009
Takashi Kobayashi	Tohoku University, Japan	Apr.2008 – Mar.2009
Kenichiro Kusudo	The University of Tokyo, Japan	Apr.2008 – Mar.2009
Hiroshi Kamata	Tokyo Institute of Technology, Japan	Apr.2008 – Mar.2009
Keita Kimura	The University of Tokyo, Japan	Apr.2008 – Mar.2009
Shun Takahashi	The University of Tokyo, Japan	Apr.2008 – Mar.2009
Lee Sang-Yoon	The University of Tokyo, Japan	Apr.2008 – Mar.2009
Yuma Okazaki	Tohoku University, Japan	Apr.2008 – Mar.2009
Naoyuki Masumoto	The University of Tokyo, Japan	Apr.2008 – Mar.2009
Yoshitaka Niida	Tohoku University, Japan	Apr.2008 – Mar.2009
Haruki Kiyama	The University of Tokyo, Japan	Apr.2008 – Mar.2009
Atsufumi Inoue	The University of Tokyo, Japan	Apr.2008 – Mar.2009
Yasushi Kanai	The University of Tokyo, Japan	Apr.2008 – Mar.2009
Tatsuki Takakura	The University of Tokyo, Japan	Apr.2008 – Mar.2009
Tomohiro Nagase	Tokyo Institute of Technology, Japan	Apr.2008 – Mar.2009

Name	Affiliation	Period
Seiichiro Kagei	Tokyo University of Science, Japan	Apr.2008 – Mar.2009
Ryota Koibuchi	Tokyo University of Science, Japan	Apr.2008 – Mar.2009
Hiroki Morishita	Keio University, Japan	Apr.2008 – Mar.2009
Sanae Iida	Keio University, Japan	Apr.2008 – Mar.2009
Hiroataka Masuyama	Tokyo University of Science, Japan	Apr.2008 – Mar.2009
Hiroaki Koguchi	Tokyo University of Science, Japan	Apr.2008 – Mar.2009
Yuuki Ichigo	Tokyo University of Science, Japan	Apr.2008 – Mar.2009
Hiroshi Takahashi	Tokyo Institute of Technology, Japan	Apr.2008 – Mar.2009
Hiroyuki Suzuki	Tokyo Institute of Technology, Japan	Apr.2008 – Mar.2009
Takayuki Yamamoto	The University of Tokyo, Japan	Apr.2008 – Mar.2009
Hiroyuki Fukasaka	Nara Institute of Science and Technology	May2008 – Feb.2009
Norihito Kitajima	The University of Tokyo, Japan	May2008 – Mar.2009
Yasuhiko Oda	The University of Tokyo, Japan	May2008 – Mar.2009
Tadakiyo Seki	Osaka University, Japan	Jul.2008 – Sep.2008
Tatsuya Kukita	Osaka University, Japan	Aug.2008 – Aug.2008
Yuuto Ueno	Hokkaido University, Japan	Aug.2008 – Aug.2008
Takayuki Watanabe	Tohoku University, Japan	Aug.2008 – Mar.2009
Makoto Igarashi	Tohoku University, Japan	Sep.2008 – Sep.2008
Tsubasa Takanami	Nagaoka University of Technology, Japan	Oct.2008 – Feb.2009
Takashi Otani	Nagaoka University of Technology, Japan	Oct.2008 – Feb.2009
Hironori Endo	Nagaoka University of Technology, Japan	Oct.2008 – Feb.2009
Kohei Morita	Kyushu University, Japan	Oct.2008 – Mar.2009
Tetsuya Miyawaki	Tohoku University, Japan	Nov.2008 – Mar.2009
Kikombo Andrew Kilinga	Hokkaido University, Japan	Dec.2008 – Mar.2009
Kohei Kawasaki	Toyohashi University of Technology, Japan	Jan.2009 – Feb.2009
Masayuki Sugawara	The University of Tokyo, Japan	Jan.2009 – Mar.2009

I . Research Topics

Overview of Research in Laboratories

Materials Science Laboratory

Keiichi Torimitsu

The aims of the Materials Science Laboratory (MSL) are to discover novel functions of materials, produce new functions and design advanced devices based on these novel functions and materials, including biological functions and materials. Our approach to accomplishing these goals involves controlling the configuration and coupling of atoms and molecules. Bio-nano research and diamond-device research constitute our principal fields of study.

We have three research groups whose work ranges from semiconductor devices, such as GaN devices, to organic materials, such as receptor proteins. The characteristic feature of the MSL is the effective sharing of unique materials and measurement techniques among the groups. This allows the fusion of research fields and techniques, which leads to innovative material research for the IT society.

We established a European laboratory in the U.K. for bio-nano research in October 2004 and thus strengthened our research activities. We promote collaboration with international organizations to develop a firm foundation of basic science.

Physical Science Laboratory

Hiroshi Yamaguchi

We are studying semiconductor and superconductor-based solid-state devices, which will have a revolutionary impact on communication and information technologies in the 21st century. In particular, we promote research of nanoscale devices fabricated using high-quality crystal growth and fine lithographic techniques.

The five groups in our laboratory are working in the following areas: precise and dynamical control of single electrons, nanodevices operating with ultra low power consumption, novel nanomechanical systems utilizing mechanical degrees of freedom in solid-state architectures, coherent quantum control of semiconductor and superconductor systems, carrier interactions in semiconductor hetero- and nanostructures, atom chips, spintronics manipulating both electron and nuclear spins. We also promote the studies of cutting-edge nanolithography techniques, high-quality crystal growth, and theoretical studies including first-principle calculations.

Optical Science Laboratory

Yasuhiro Tokura

This laboratory aims for the development of core-technologies that will innovate on optical communications and optical signal processing, and seeks fundamental scientific progresses.

The groups in our laboratory are working for the quantum state control by very weak light, the search for intriguing phenomena using very intensive and short pulse light, and very small optical integrated circuits using two-dimensional photonic crystals, based on the optical properties of semiconductor nanostructures like a quantum dot.

In this year, we realized improvements of quality of entangled photon pairs from silicon wire waveguide, magneto-optical spectroscopy of charged excitons and trions in quantum dots, and short pulse generation by adiabatic wavelength tuning in a photonic crystal high- Q cavity.

Boron-Implanted Diamond FETs Formed by Ion-Implantation and High-Pressure and High-Temperature Annealing

Kenji Ueda and Makoto Kasu
Materials Science Laboratory

Ion implantation is a widely used doping technique for Si and GaAs. However, in the case of diamond, implantation-induced damage cannot be recovered by conventional thermal annealing because its annealing condition is not located in diamond stable phase but in graphite stable phase. Previously, we reported that high pressure and high-temperature (HPHT) annealing in diamond stable phase is highly effective to recover damages induced during ion-implantation [1]. In this study, we achieved higher hole concentration and mobility using this technique and successfully fabricated diamond FETs [2].

CVD homoepitaxial diamond films were grown on Ib (100) substrates by microwave plasma CVD. Then, boron (B) ions were implanted in the films at an acceleration energy of 60 keV with a dose of $10^{15}\sim 10^{16}$ cm⁻². HPHT annealing of the B-implanted films was performed at ~ 7 GPa and 1350°C for activation of dopants. Using these diamond films, FETs were fabricated (Fig. 1). The source and drain contacts were formed by Ti/Au with annealing at 600°C. The Schottky-gate contact was formed by the evaporation of Al.

We obtained a higher hole concentration for a dose of $1\sim 5\times 10^{15}$ cm⁻² while keeping high mobility. For a dose of 3×10^{15} cm⁻², we obtained sheet concentration and mobility at 300 K of 1.6×10^{13} cm⁻² and 41 cm²/Vs, respectively. These values are comparable to those of H-terminated diamond ($\sim 10^{13}$ cm⁻² and ~ 100 cm²/Vs) widely used so far. Using this film with a dose of 3×10^{15} cm⁻², we fabricated FETs. The gate length and the width were 2 μ m and 100 μ m, respectively. Current saturation and pinch-off characteristics were clearly observed. The maximum I_{DS} of 0.15 mA/mm was obtained at V_{GS} of -2 V (Fig. 2). The forward breakdown voltage (V_{BR}) of the FET was 530 V. Breakdown of the point was destructive and part of Al Schottky and Au/Ti ohmic electrodes melted. The breakdown electric field was estimated to be ~ 1.1 MV/cm. The E_c is comparable to those of Al-Schottky diodes using B-doped CVD homoepitaxial diamond films [1, 2]. The result also indicates the high quality of our B-implanted layers.

This work was partly supported by the SCOPE project of the Ministry of Internal Affairs and Communications, Japan.

[1] K. Ueda, M. Kasu, and T. Makimoto, Appl. Phys. Lett. **90** (2007) 122102.

[2] K. Ueda and M. Kasu, Physica Status Solidi (c) **5** (2008) 3175.

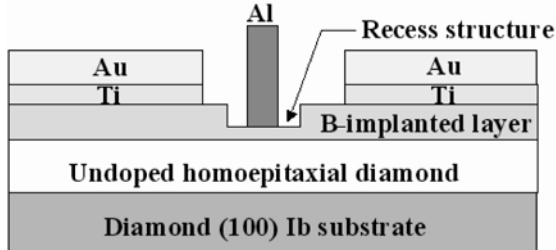


Fig. 1. Schematic cross-section of B-implanted diamond FET.

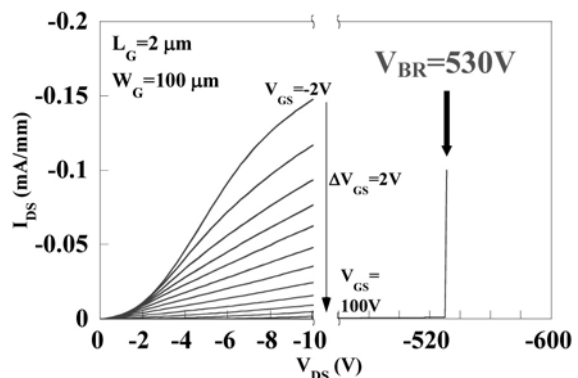


Fig. 2. DC drain current voltage characteristics for the B-implanted diamond FETs.

High Performance Nitride-Based Heterojunction Bipolar Transistors on GaN Substrates

Kazuhide Kumakura and Toshiki Makimoto
Materials Science Laboratory

There are large mismatches between III-nitride semiconductors and conventionally used sapphire substrates in terms of the lattice constant or thermal expansion coefficient. Therefore, the most suitable substrate for GaN growth is no doubt the GaN substrate. From the viewpoints of device applications, the merits of using GaN substrates are as follows: a low dislocation of the substrate itself, resulting in improving the device performance, or a relatively large thermal conductivity, making it possible to spread heat generated under a high-power operation. In principle, heterojunction bipolar transistors (HBTs) have the ability to operate with uniform threshold voltages and high current densities. A normally off characteristic is advantageous for a fail-safe system. Therefore, nitride-based HBTs are one of the attractive devices for high-power electronics. In this work, we fabricated the *pnp* AlGaIn/GaN HBTs on GaN substrates and showed their high performance at room temperature (RT).

Figure 1 shows current gains as a function of the collector current (I_c) of *pnp* AlGaIn/GaN HBTs on sapphire and GaN substrates measured at RT. The HBTs on GaN substrates exhibited a high performance: a maximum current gain of 85 at a collector current of 30 mA and a maximum collector current density of 7.3 kA/cm² at a collector-emitter voltage of 30 V, which corresponds to the maximum power dissipation density of 219 kW/cm². The current gain and the collector current density increased compared to those on sapphire substrates. The calculated minority carrier diffusion length agreed well with that determined from electron beam induced current measurements [1]. Therefore, these results indicate that the current gain was dominated by the minority hole diffusion in the neutral base at high I_c for the HBTs on the GaN substrates, and that the increase in the current gain is ascribed to the low dislocation density in the HBTs. For the HBT with the large emitter area, the current gain was still as high as 47 and the maximum collector current reached as high as 1 A, and this single HBT showed a high-power dissipation of 30 W as shown in Fig. 2. This high performance of the HBTs is ascribed to the low dislocation density and relatively high thermal conductivity of the GaN substrate.

[1] K. Kumakura et al., Appl. Phys. Lett. **86** (2005) 052105

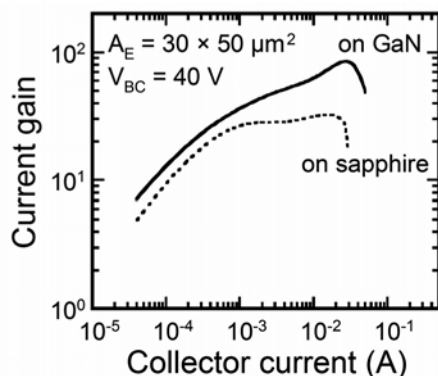


Fig. 1. Current gain as a function of collector current of the HBTs measured at RT. The solid and broken lines correspond to the data for HBTs on GaN and sapphire substrates, respectively.

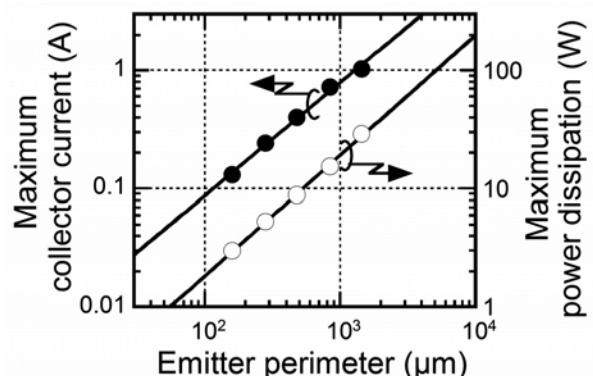


Fig. 2. Maximum collector current and the maximum power dissipation as a function of the emitter perimeter of the HBTs on GaN substrates.

Anisotropic In-Plane Strains in Non-Polar $\text{Al}_{1-x}\text{Ga}_x\text{N}$ ($\bar{1}\bar{1}20$) Films ($x < 0.2$)

Tetsuya Akasaka, Yasuyuki Kobayashi, and Makoto Kasu
Materials Science Laboratory

Nitride semiconductor films with non-polar faces, such as $(\bar{1}100)$ and $(\bar{1}\bar{1}20)$ faces, are attracting much attention, because emission efficiency of quantum wells using the non-polar faces is higher than those using polar faces, such as (0001) face, by the elimination of piezoelectric polarization fields [1]. On the other hand, SiC has been widely used as the substrate for heteroepitaxy of nitride semiconductors, because of its high electrical and thermal conductivities and the smaller lattice mismatches ($\sim 1\%$ for AlN). However, there is anisotropy in the lattice mismatches between nonpolar nitride semiconductors and SiC substrates and the lattice matching of the heteroepitaxy is complicated. For example, the a - and c -axes of AlN are 1.05% longer and 1.13% shorter than those of SiC, respectively. In this study, we have grown $\text{Al}_{1-x}\text{Ga}_x\text{N}$ ($\bar{1}\bar{1}20$) thin films ($x < 0.2$) on SiC ($\bar{1}\bar{1}20$) substrates and evaluated the lattice constants, in-plane strains and crystallinity of the films.

The pseudomorphic growth (lattice-matched with substrate) is essential for heteroepitaxy for reducing the densities of dislocations and stacking faults. Figure 1 shows dependence of in-plane strains in $\text{Al}_{1-x}\text{Ga}_x\text{N}$ ($\bar{1}\bar{1}20$) thin films on the Ga composition. The in-plane strains along the $[\bar{1}100]$ and $[0001]$ directions, ϵ_{xx} and ϵ_{zz} , are on the pseudomorphic lines at the Ga compositions lower than 0.06, which means that the in-plane lattice constants of the films are almost the same as those of SiC. This pseudomorphic growth is successfully achieved by balance between compressive stress along $[\bar{1}100]$ and tensile one along $[0001]$ [2]. Dependence of full width at half maximum (FWHM) of $(\bar{1}\bar{1}20)$ X-ray rocking curves (XRC) is plotted as a function of the Ga composition in Fig. 2. The tilt angle toward $[0001]$, tilt $[0001]$, which is related to the density of stacking faults parallel to the (0001) plane, decreases by increasing the Ga composition. This is because the in-plane strain along the $[0001]$ direction, ϵ_{zz} , decreases by increasing the Ga composition (see Fig. 1).

The pseudomorphic growth of $\text{Al}_{1-x}\text{Ga}_x\text{N}$ ($\bar{1}\bar{1}20$) thin films ($x < 0.06$) are achieved in this study. In addition, our findings can provide a basic guideline for the design of nonpolar light-emitting devices, because both the band structures and the polarization of the emitted lights can be modified by anisotropic strains.

[1] P. Waltereit et al., Nature **406** (2000) 865.

[2] T. Akasaka, Y. Kobayashi, and M. Kasu, Appl. Phys. Lett. **93** (2008) 161908.

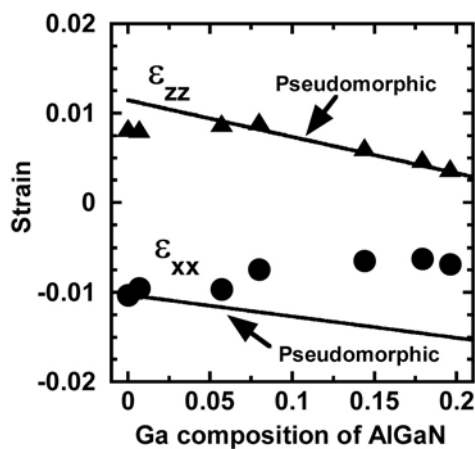


Fig. 1. In-plane strains along the $[\bar{1}100]$ direction, ϵ_{xx} (●) and along the $[0001]$ direction, ϵ_{zz} (▲) plotted as a function of the Ga composition.

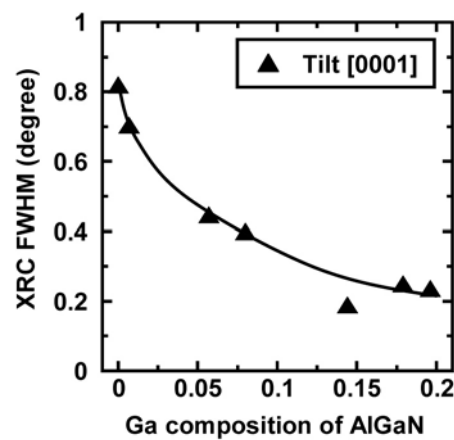


Fig. 2. Tilt angle along the $[0001]$ direction plotted as a function of the Ga composition.

Molecular Beam Epitaxial Growth of Hexagonal Boron Nitride on Ni(111) Substrate

Chiun-Lung Tsai, Yasuyuki Kobayashi, and Tetsuya Akasaka
Materials Science Laboratory

Hexagonal boron nitride (*h*-BN), with its wide bandgap in the deep ultraviolet region, has been gaining interest since it was proposed as a promising material for optoelectronic applications. The *h*-BN epitaxial growth has been achieved using the metalorganic vapor phase epitaxy (MOVPE) [1]. Parasitic reactions between sources in BN epitaxy by MOVPE can be avoided in molecular beam epitaxy (MBE) growth of *h*-BN. However, a polycrystalline BN structure was obtained by MBE and no successful MBE-grown *h*-BN epitaxy has been reported yet.

Here, we report the epitaxial *h*-BN growth on Ni(111) substrate by MBE [2]. Elemental boron evaporated by an electron-beam gun and active nitrogen generated by a radio-frequency (RF) plasma source were used as the group-III and -V sources, respectively. Figure 1 shows in-situ reflection high energy electron diffraction (RHEED) pattern taken along the $[\bar{1}10]$ azimuth of Ni(111) surface at the end of 1000 Å BN growth. The unreconstructed intense streaky (1×1) patterns were seen immediately upon initiation of the MBE growth of BN, and the consistent streaky (1×1) pattern was recorded during the entire process till the end of 1000 Å BN growth. The streaky patterns observed throughout the entire growth carried out at a relatively low temperature of 890°C not only indicate the formation of single-crystalline BN, but also mean the growth proceeded with a smooth growth front.

A representative XRD for the 1000 Å *h*-BN epitaxial film is shown in Fig. 2. Diffraction peaks from both the *h*-BN(0002) and *h*-BN(0004) planes along with the underlying Ni(111) substrate prove the formation *h*-BN with the orientation of *h*-BN[0001] parallel to the Ni[111] direction. The inset of Fig. 2 shows the x-ray rocking curve of the *h*-BN epitaxial film characterized by the full width at half maximum (FWHM) of 0.61°. This FWHM from a 1000 Å film is narrower than the best value ever reported [1], and can possibly be further decreased by optimizing the growth conditions and/or increasing the epitaxial film thickness. From the RHEED observation and XRD, the alignments between the *h*-BN film and the Ni substrate are $[0001]_{h\text{-BN}} \parallel [111]_{\text{Ni}}$, $[11\bar{2}0]_{h\text{-BN}} \parallel [\bar{1}10]_{\text{Ni}}$ and $[1\bar{1}00]_{h\text{-BN}} \parallel [\bar{1}\bar{1}2]_{\text{Ni}}$. The achievement of *h*-BN epitaxial growth by MBE allows us to clarify fundamental properties, such as near-band-gap luminescence.

[1] Y. Kobayashi et al., J. Crystal Growth **298** (2007) 325.

[2] C.L. Tsai et al., J. Crystal Growth (in press).

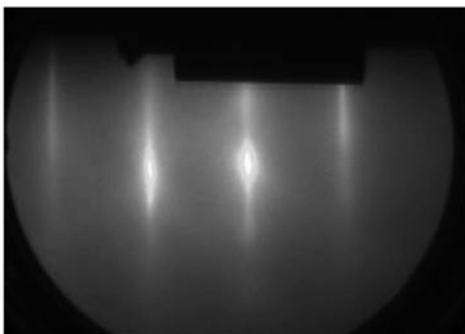


Fig. 1. The RHEED pattern at the end of 1000 Å BN growth.

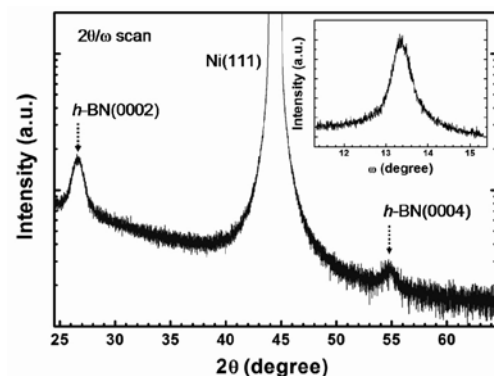


Fig. 2. The 2θ/ω XRD of the *h*-BN epitaxial film with an inset displaying the XRC.

Simultaneous Optical and Electrical Characterization at Nanoscale with Scanning Probe Microscope

Hiroo Omi, Ilya Sychugov, and Yoshihiro Kobayashi
Materials Science Laboratory

Optical and electrical properties of nanostructures can be addressed using electromagnetic radiation or electrical current as a probe. In general, a near-field type of electromagnetic interaction is necessary for an optical probe to enter nanoscale regime in spatial resolution by overcoming the optical diffraction limit ($\sim 1 \mu\text{m}$). A typical aperture scanning near-field optical microscope (aperture-SNOM) provides such an opportunity both for the excitation and collection of light. However, this instrument employs a dielectric fiber tip as an aperture, which makes it unsuitable for electrical measurements. An apertureless SNOM, on the contrary, has a metallic, needle-like opaque tip. The local field enhancement at the tip apex due to the plasmon effect enhances signal in the light scattering experiments. But, unlike the case of aperture-SNOM, the far-field optics alignment is necessary and the scattered light from the tip shaft can distort the measurements. In addition, the aperture-SNOM can operate in the combination with a scanning tunnelling microscope (STM) and it was demonstrated that such a combination can yield superior resolution for SNOM imaging compared to the conventional shear-force approaching method. On the other hand, the STM, which is capable of atomic-resolution measurements using electrical current, can also cause an optical response in materials. The collection of light in ordinary STM machines with opaque metal tips is realized by far-field optics. When the carriers are tunnelled to the sample it is the excitation (tunnelling) area that limits the spatial resolution; the achieved resolution of such an instrument was reported to be as small as $\sim 10 \text{ nm}$. The collection efficiency of the emitted light can be improved by employing a transparent STM tip, where the light is coupled directly to the tip rather than to a far-field detector. However, only the electrical probing of nanostructures was proven feasible in such a scanning tunnelling microscope luminescence (STML) experiment. We expand the STML approach to show an ultimate STM-based configuration with the aperture metal tip (Fig. 1), where both optical and electrical excitations are available (Fig. 2). This method enabled us to characterize the same area in near-field of the sample through the aperture of transparent tip covered with metals [1].

[1] I. Sychugov, H. Omi, T. Murashita, and Y. Kobayashi, *Nanotechnology* **20** (2009) 145706.

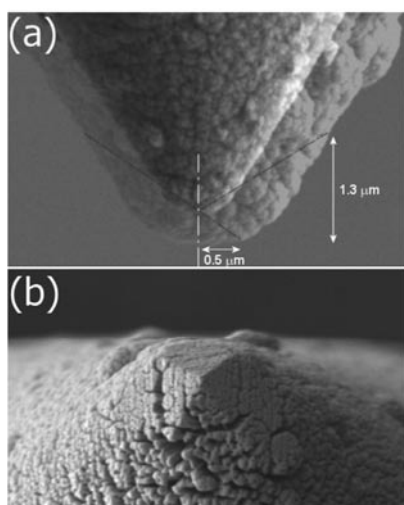


Fig. 1. Aperture metal tip.

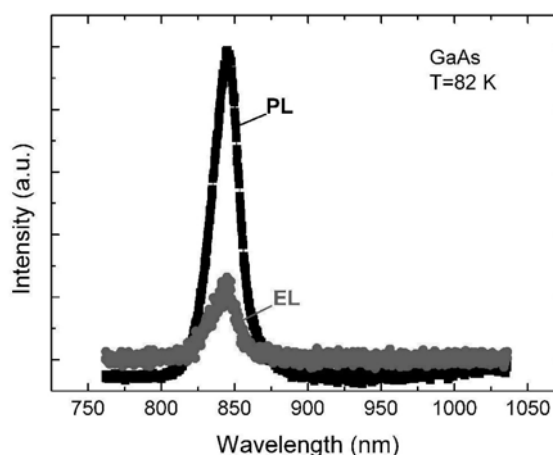


Fig. 2. Electro- and photoluminescence from the GaAs wafer on a nanoscale.

Diameter Dependence of Hydrogen Adsorption on Single-Walled Carbon Nanotubes

Akio Tokura¹, Fumihiko Maeda¹, Yuden Teraoka², Akitaka Yoshigoe², Daisuke Takagi³,
Yoshikazu Homma³, Yoshio Watanabe⁴, and Yoshihiro Kobayashi¹

¹Materials Science Laboratory

²Synchrotron Radiation Research Center, Japan Atomic Energy Agency

³Department of Physics, Tokyo University of Science and CREST-JST

⁴Japan Synchrotron Radiation Research Institute

Single-walled carbon nanotubes (SWNTs) are of great interest as a promising material for a new generation of electronics. Controlling their properties is an important challenge. Because the properties deeply depend on the SWNT structure, surface modification is suitable for such control. Additionally, selecting reactions in SWNTs is attractive as a way to extract nanotubes having desirable properties. It has been predicted theoretically that C-H bonds are stable for small-diameter SWNTs [1], and that the band-gap modulation depends on the coverage of hydrogen [2]. In this work, we investigated the adsorption of atomic hydrogen on SWNTs with the aim of controlling SWNT properties through surface modification.

In situ core level photoelectron spectroscopy (PES) was used for the chemical analysis, and *ex situ* Raman spectroscopy was used for the structural deformation analysis. By fitting the C1s core level spectrum captured after atomic hydrogen irradiation, we found the C-H bonds in the nanotubes as shown in Fig. 1. Before and after PES measurement, Raman spectra were captured as shown in Fig. 2. The spectra demonstrate that, by the irradiation, the radial-breathing-mode (RBM) intensity of small-diameter SWNTs (less than about 1.2 nm in this work) is severely decreased compared to that of large-diameter SWNTs. Raman spectroscopy results indicate adsorption-induced bonding-structure deformation is generated more easily on small-diameter SWNTs. Taken together, these results indicate that hydrogen atoms adsorb more preferentially on SWNTs with small diameters [3]. Our results suggest that SWNT properties can be modified selectively by controlling hydrogen adsorption.

[1] T. Yildirim et al., Phys. Rev. B **64** (2001) 075404.

[2] K. A. Park et al., J. Phys. Chem. B **109** (2005) 8967.

[3] A. Tokura et al., Carbon **46** (2008) 1903.

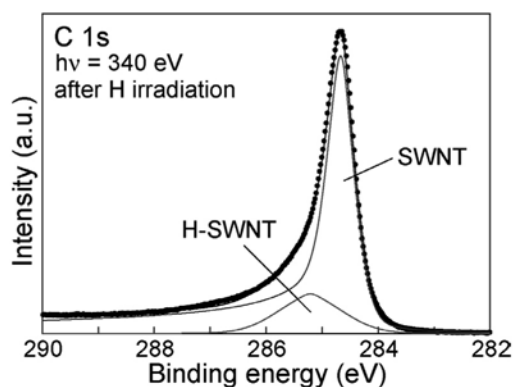


Fig. 1. Peak fitting result of C1s spectrum of SWNT sample captured after hydrogen irradiation.

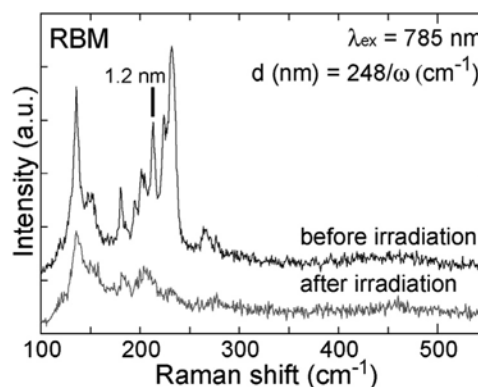


Fig. 2. Raman spectra in the RBM region of SWNT sample captured before and after hydrogen irradiation.

Number-of-Layers Dependence of Electronic Properties of Epitaxial Few-Layer Graphene

Hiroki Hibino, Hiroyuki Kageshima*, and Fumihiko Maeda
Materials Science Laboratory, *Physical Science Laboratory

Graphene is attracting intense attention as a future electronic material due to its superior electronic transport properties. Epitaxial few-layer graphene (FLG) grown on SiC by thermal decomposition can be easily scaled-up and is promising for device integration. However, it is still difficult to grow epitaxial FLG to an intended thickness. To overcome this problem, we have developed a method for evaluating the number of graphene layers N_G in epitaxial FLG microscopically using low-energy electron microscopy (LEEM) and have used it to control the growth [1]. For device applications of epitaxial FLG, it is also important to clarify how the SiC substrate influences the electronic properties of FLG. The influence of the substrate results in the N_G dependence of the electronic properties, which was investigated using spectroscopic photoemission and LEEM (SPELEEM) at SPring-8 [2].

Figure 1 shows photoemission electron microscopy (PEEM) images of epitaxial FLG grown on 6H-SiC(0001). The PEEM images were made by secondary electrons (SEs) emitted under irradiation of photons of 400 eV. Numbers indicated in (b) are N_G values determined by LEEM. Areas with different N_G can be discriminated in the SE PEEM images, but their relative intensities depend on the SE energy. Figure 2 shows the SE emission spectra obtained from the sequential SE PEEM images at different energies. The SE emission spectra depend on N_G in two aspects; the threshold start voltage of the SE emission and the spectrum shape. The threshold voltage corresponds to the vacuum level. Monolayer graphene has a work function about 0.3 eV smaller than bulk graphite, and the work function of epitaxial FLG increases with N_G . The N_G dependence of the spectrum shape is explained by unoccupied electronic states in epitaxial FLG discretized due to its finite thickness. Similar experiments for C1s core level photoelectrons indicated that the C1s binding energy also depends on N_G . The N_G dependences of the work function and C1s binding energy are consistent with the shift of the electronic structure of epitaxial FLG caused by the electron doping from the SiC substrate [3].

- [1] H. Hibino et al., Phys. Rev. B **77** (2008) 075413; H. Hibino et al., e-J. Surf. Sci. Nanotechnol. **6** (2008) 107.
[2] H. Hibino et al., Phys. Rev. B **79** (2009) 125437.
[3] T. Ohta, A. Bostwick, T. Seyller, K. Horn, and E. Rotenberg, Science **313** (2006) 951.

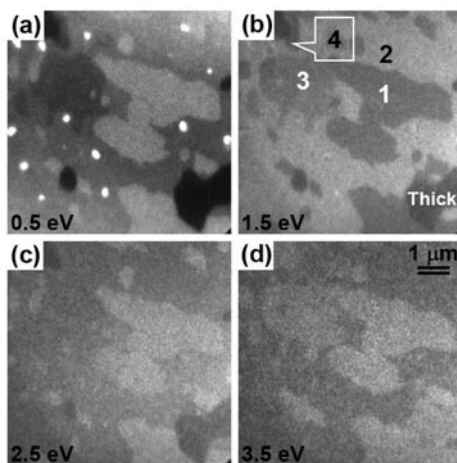


Fig. 1. SE PEEM images of epitaxial FLG grown on 6H-SiC(0001).

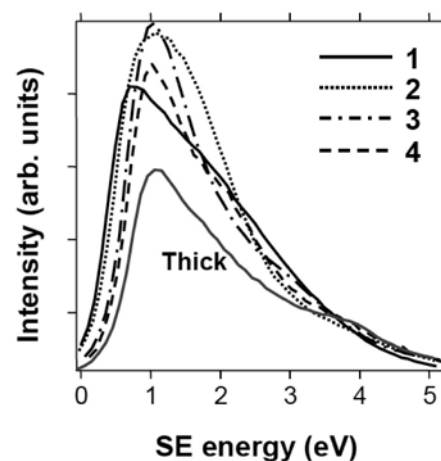


Fig. 2. SE emission spectra of epitaxial FLG obtained from the sequential SE PEEM images.

Precise Control of Gold Nanorod Arrays

Hiroshi Nakashima
Materials Science Laboratory

Gold nanorods have a fascinating optical property, whose origin is localized surface plasmon resonance, and this property is dependent on their structural aspect ratio [1]. Gold nanorods assembled on a solid surface exhibit unique optoelectronic properties arising from collective interactions in an ordered state, and these properties make it possible to incorporate nanomaterials into nanophotonic, electronic devices, and biosensors. Here we synthesize novel gold nanorods coupled with thiol-terminated lipids (Fig. 1). We use a controlled self-assembly process to achieve precise control of the structures of the gold nanorod arrays including their structural dimensions, orientation and particle gap distance [2].

The lipid modified gold nanorods form 1D ordered structures with side-to-side configurations on a Si substrate, that are induced by the self-assembly of lipids during the drying process [Fig. 2(a)]. The distance between neighboring nanorods is uniform at 5.0 nm, which is to the same as the thickness of the lipid bilayer. Interestingly, high-density nanorod composites exhibit an extensive 2D self-assembly. Furthermore, we observe anisotropically oriented nanorods in a 2D assembly that are dependent on the nature of the Si surface. On a hydrophilic Si surface, the nanorods are organized laterally in relation to the substrate [Fig. 2(b)]. In contrast, on a hydrophobic Si surface, the nanorods are perpendicular to the substrate [Fig. 2(c)]. As regards the 2D self-assembly of the nanorods, our results constitute the first example of the precise control of the interparticle spacing and of anisotropic orientation in a lateral or perpendicular fashion dependent on the interfacial hydrophilicity or hydrophobicity.

The lipid modified gold nanorod is a biocompatible nanomaterial. Therefore, various biomolecules such as membrane proteins, enzymes and antibodies can be attached to the nanorod surface and function while retaining their physiological properties. The gold nanorod array on a solid surface will be utilized for surface enhanced Raman scattering or fluorescence substrates. Our future goal is to use the gold nanorod array to develop highly sensitive biochips that can detect intermolecular interactions on a single (bio)molecular scale.

[1] D. P. Sprünken et al., *J. Phys. Chem. C* **111** (2007) 14299.

[2] H. Nakashima et al., *Langmuir* **24** (2008) 5654.

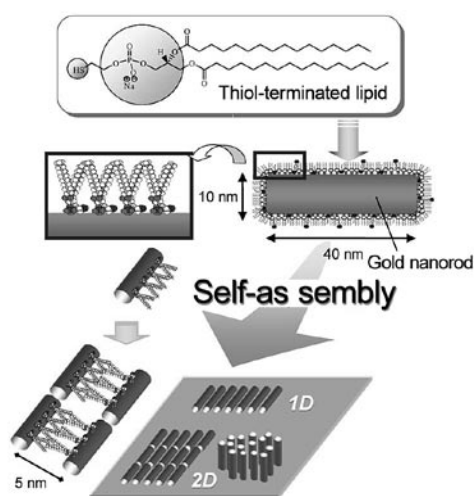


Fig. 1. Lipid modified gold nanorods and their self-assembled structures.

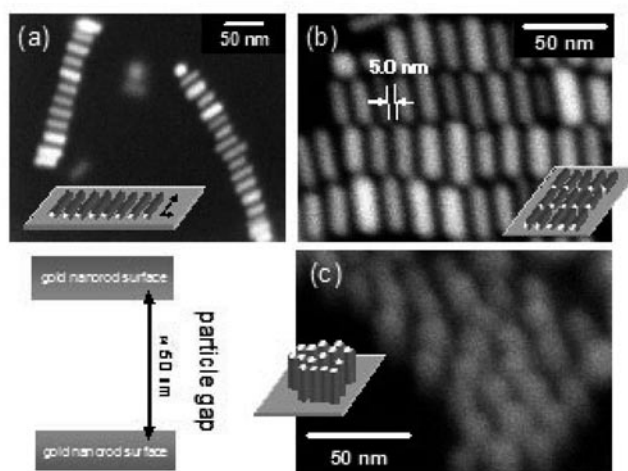


Fig. 2. Gold nanorod arrays with (a) 1D, (b) 2D lateral, and (c) 2D perpendicular configurations.

Observation of Ligand-Induced Conformational Changes in Single ATP Receptors with Fast-Scanning Atomic Force Microscopy

Youichi Shinozaki¹, Koji Sumitomo¹, Makoto Tsuda², Schuichi Koizumi³,
Kazuhide Inoue², and Keiichi Torimitsu¹

¹Materials Science Laboratory, ²Kyushu University, ³Yamanashi University

Proteins, known as "receptors" that exist in cells, exhibit their functions via binding with small compounds such as hormones. When the receptor is a type of ion channel, it opens its pore after binding with compounds thereby flowing ions through it and resulting in exhibiting its function. We observed the topology and stimulation-induced conformational changes in adenosine triphosphate (ATP) receptor [1], an important receptor in pain sensation, with atomic force microscopy (AFM).

ATP receptor gene was over-expressed in immortalized cells. ATP receptor proteins were purified from their cell membranes and receptors for AFM observation were adsorbed on freshly cleaved mica. Non-stimulated ATP receptor exhibited circular feature and that after ATP stimulation was in tripartite morphology (Fig. 1). To study whether structural difference between these two state is derived from the stimulation-induced conformational change in ATP receptor, we performed time-lapse imaging of conformational changes in ATP receptor with fast-scanning AFM. Before stimulus, ATP receptor exhibited circular feature (Fig. 2, -2.5~0.0 s). After stimulus, ATP receptor immediately changed its structure into trimeric topology (Fig. 2, 0.5 s). Detailed analysis of trimeric ATP receptor revealed that it exhibited the further disengagement of three subunits and large pore-like structure in its center (Fig. 2, 2.0~5.0 s). To confirm whether these structural changes are related to the physiological functions, we measured permeability of ATP receptor channel using fluorescent molecules. ATP receptor exhibited permeability to calcium ions and appeared to be functional. When imaging buffer contains no calcium, ATP receptor exhibited permeability to larger molecules (ethidium bromide) but not when imaging buffer contains calcium. These results indicate that structural changes in ATP receptor appeared to correspond to the physiological function via flowing ions through its pore. Thus, we succeeded in observation of topology and structural changes related to physiological functions of ATP receptor. We will reconstitute receptors into artificial lipid bilayer on a flat substrate [2] and analyze the relationship of receptor-lipid interaction and receptor topology/function.

[1] Y. Shinozaki et al., PLoS Biol. (accepted).

[2] Y. Shinozaki et al., Jpn. J. Appl. Phys. **47** (2008) 6164.

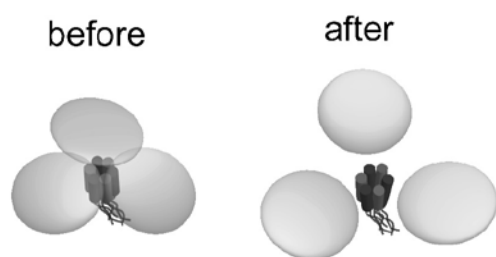


Fig. 1. Schematics of ATP receptors before (left) and after (right) stimulation.

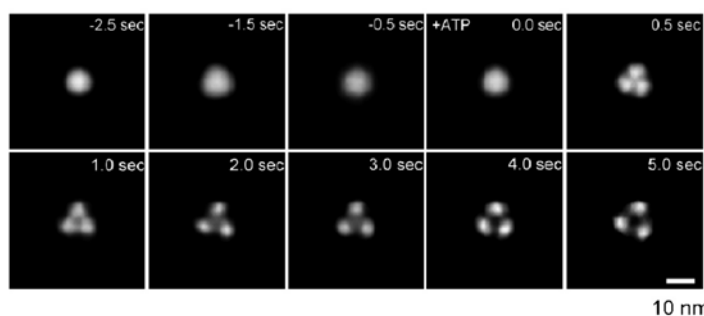


Fig. 2. Time-lapse imaging of stimulation-induced conformational changes in ATP receptor.

The Preferential Reconstitution of Receptor Proteins into Model Lipid Domains Studied by Atomic Force Microscopy

Nahoko Kasai, Chandra S. Ramanujan*, Kamal Marwaha*,
John F. Ryan*, and Keiichi Torimitsu
Materials Science Laboratory, *University of Oxford

Receptor proteins play a fundamental role in biological membranes. They bind to ligand molecules and transfer signals into the cells by means of electricity and by chemical modification of proteins. Biological membranes are principally made of lipid molecules. Recent studies have revealed that lipid membrane in the synaptic junctions of central nervous system (CNS) is heterogeneous in composition and consists of small regions known as rafts [1]. These raft-like domains are loci for insertion of receptor proteins and are believed to act as signalling platforms that organize and compartmentalize receptor proteins to modify the synaptic signalling.

We report atomic force microscopy (AFM) measurements of the glutamate receptors (GluRs), the most common membrane receptor proteins found in the CNS. GluRs are implicated in learning and memory, and up-regulation of its numbers in the post-synaptic membrane possibly being a key component of this process. In this work we have investigated the dependence of protein reconstitution in model membranes on lipid composition.

We reconstituted purified GluRs into a lipid mixture system consisting of a mixture that makes up approximately 60% of the synaptic membrane. As shown in Fig. 1, the mixture formed two distinct domains when immobilized on mica: a high domain (HD) at 7 nm height and a low domain (LD) at 5 nm. The lateral extent of HD is typically ~ 100 nm, which has structural similarities with the raft-like domains in synaptic membranes, albeit with much simpler composition. Then we reconstituted GluRs and found that the receptors preferentially insert into the HD comparing to the LD as shown in Fig. 2 [2]. This result demonstrates that bilayer thickness is a significant factor in the membrane self-assembly process. This can be expected to reveal signalling mechanism in synapses.

This research was supported in part by Bio-nanotechnology IRC in UK and by the Strategic International Cooperative Program, Japan Science and Technology Agency (JST).

[1] J. A. Allen et al., *Nat. Rev. Neurosci.* **8** (2007) 128.

[2] C. S. Ramanujan et al., 52nd Biophys. Soc. Meeting Abst. (2008) B363.

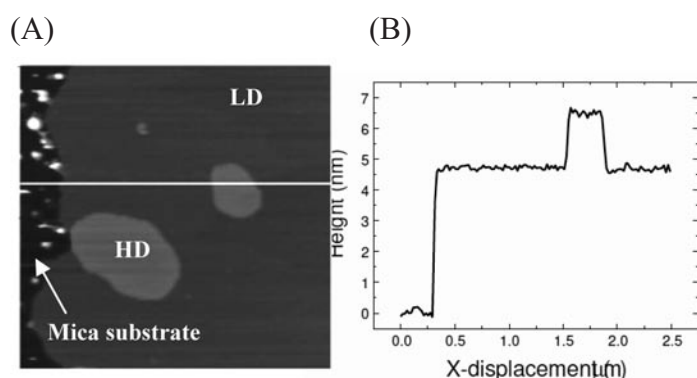


Fig. 1. (A) AFM image of raft-like domains in lipid membrane on mica ($2.5 \mu\text{m}$ square) and (B) height profile.

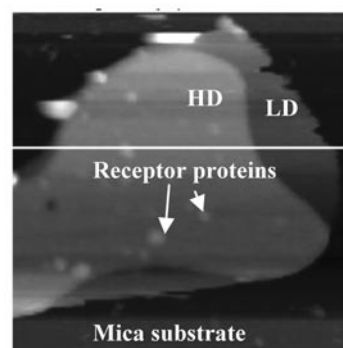


Fig. 2. AFM image of lipid domain with reconstituted membrane proteins ($1 \mu\text{m}$ square).

Effect of Nanogap on Dynamics of Lipid Bilayer

Yoshiaki Kashimura and Kazuaki Furukawa
Materials Science Laboratory

Cell membranes play an important role in the activity of bio-molecules, for example, membrane proteins. A lipid bilayer, which is a basic component of a cell membrane, can be fabricated artificially on a hydrophilic surface by spontaneous growing characteristic (self-spreading). Such membranes remain the fluidity based on lateral diffusion. Using these characteristics, in this study, we investigated the dynamics of a lipid bilayer on a nano-patterned surface and the molecular transport using the lipid bilayer as a molecule carrier [1].

L- α -Phosphatidylcholine (extracted from egg yolk) containing 5 mol% of dye-conjugated lipid was prepared. Dyes used were Texas Red, fluorescein and NBD with different molecular size. Nanogap (10~200 nm) using Au was fabricated on an SiO₂ surface. Microchannel that had wells at both ends was fabricated on this nanogap structure using a photoresist [Fig. 1(a)]. A small amount of a lipid source was adhered inside the well. The self-spreading of a single lipid bilayer was initiated by immersing the device in a buffer solution. Fluorescence from the lipid bilayer was observed by a confocal laser scanning microscope.

Figure 1(b) shows a time evolution of a self-spreading lipid bilayer before and after passage through a nanogap. The single lipid bilayer developed along a microchannel and successfully passed through the nanogap without development on photoresist and gold pattern. Figure 2 shows a fluorescence image and corresponding fluorescence intensity profile obtained after a sufficient time interval. This result clearly shows that the fluorescence intensity decreases discontinuously in the vicinity of the nanogap. This behavior strongly depends on the size of the nanogap and dye moiety. The dye molecules experience interference when they pass through the nanogap although the nanogap size is much larger than that of the dye moiety (at most 3 nm).

[1] Y. Kashimura et al., *Jpn. J. Appl. Phys.* **47** (2008) 3248.

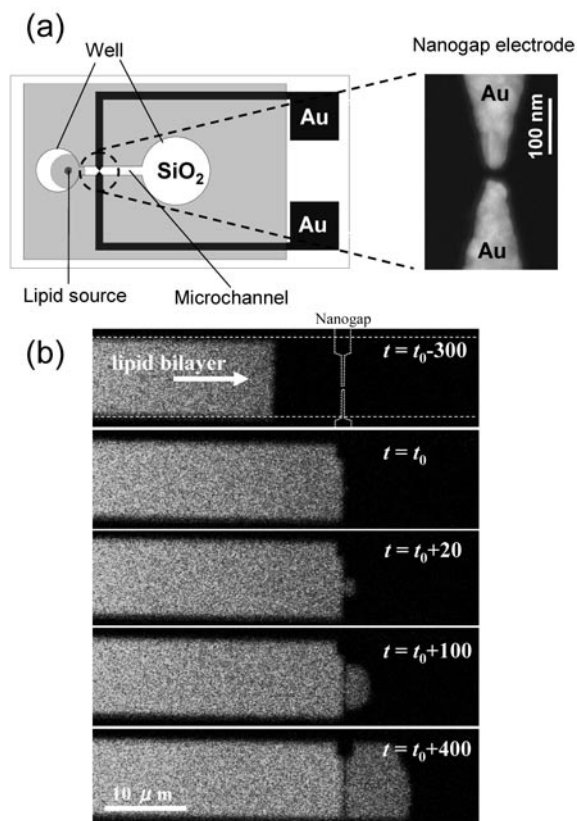


Fig. 1. (left) (a) Device structure used in this study. (b) Time evolution of the self-spreading lipid bilayer. The time at which an advancing lipid bilayer reaches a nanogap is set at $t=t_0$ s.

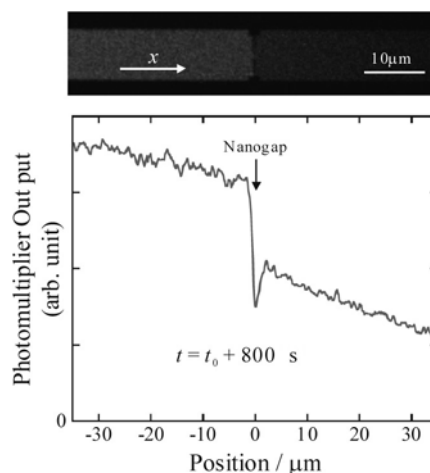


Fig. 2. Fluorescence image and fluorescence intensity profile after a sufficient time interval.

Stochastic Data Processing Based on Single Electrons Using Nano Field-Effect Transistors

Katsuhiko Nishiguchi, Yukinori Ono, and Akira Fujiwara
Physical Science Laboratory

Although the miniaturization of Si metal-oxide-semiconductor field-effect transistors (MOSFETs) continues to improve the performance of various consumer electronics, the need to guarantee error-free operation of MOSFETs makes it difficult to reduce supply voltage, which leads to ever increasing current density and power consumption. In this work, conversely, we reduce the current density of nanoscale FETs ultimately and then utilize its shot noise to realize a stochastic data processing for pattern recognition with high flexibility [1].

The device is composed of two transistors fabricated on a silicon-on-insulator wafer (Fig. 1). The first transistor (T-FET) has a two-layer gate: an upper gate (UG) is used to induce an inversion layer and a lower gate (LG) forms an energy barrier in the undoped channel of T-FET. As a result, an electron-storage node (MN) electrically isolated from an electron source (ES) is formed. The two layer gate can eliminate undesired leakage current originating from p - n junctions, which is a well-known issue in conventional FETs [1, 2]. Therefore, highly controllable single-electron transfer from the ES to the MN can be achieved using the LG. The single electrons transferred to the MN are detected by the other transistor (D-FET) as shown in Fig. 2. The optimization of the device structure and operation conditions allows single-electron detection even at room temperature [3]. As analysis of the time interval δt of each electron transfer to the MN revealed that the single-electron transfer is based on a Poissonian process (inset of Fig. 2), which corresponds to the real-time monitoring of shot noise in FETs with single-electron resolution.

The Poissonian stochastic behavior of such single-electron transfer can be applied to a stochastic data-processing circuit for image-pattern recognition. The circuit recognizes the input pattern as one of the reference patterns with probability correlating to the similarity between the reference and input patterns as shown in Fig. 3. Such probability can be electrically controlled by the LG. These features allow flexible pattern recognition especially for corrupted input patterns, which promises to apply high time and power efficiency to the circuit like in the human brain.

- [1] K. Nishiguchi et al., *Appl. Phys. Lett.* **92** (2008) 062105.
 [2] K. Nishiguchi et al., *IEEE Electron Device Lett.* **28** (2007) 48.
 [3] K. Nishiguchi et al., *Jpn. J. Appl. Phys.* **47** (2008) 8305.

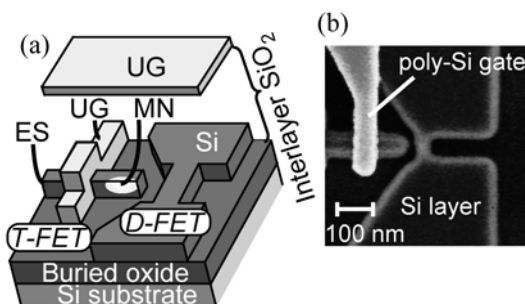


Fig. 1. Device structure based on Si transistors. (a) Schematic view. (b) Scanning electron microscope.

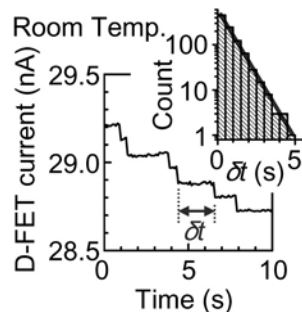


Fig. 2. Real-time monitoring of single-electron transfer. Inset: Histogram of the time interval between each single-electron transfer to the MN.

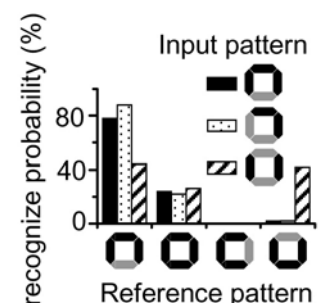


Fig. 3. Stochastic pattern recognition. The reference pattern most similar to the input pattern is selected.

Identification of Single Dopant Position in Silicon Nanotransistor

Yukinori Ono, Mohammed A. H. Khalafalla, Katsuhiko Nishiguchi, and Akira Fujiwara
Physical Science Laboratory

Future nanoscale field-effect transistors are expected to be fatally sensitive to electronic charges of a small number of dopants in the channel. On the other hand, there are reports of emerging devices using dopant atoms as functional part, such as quantum dots, for the manipulation of electronic charges. It is therefore important to establish a technology for detecting and controlling the dopant charges. We have so far reported the detection of single boron atoms in nanoscale silicon transistors [1]. Here, we report the measurements and analysis for identifying the depth position of observed single boron atoms [2].

Nano transistors whose gate length is 40 nm were fabricated on a silicon-on-insulator substrate [3]. The transistors comprise the channel lightly doped with boron, p-type source/drain, and electrically formed leads inserted between the channel and the source/drain. The insertion of the leads prevents dopant diffusion from the source/drain and enables us to investigate the conductance of the channel containing only a few dopant atoms. The conductance G was measured at 6 K. Figure 1 shows the contour plot of $d\text{Log}G/dV_F$ as a function of the front-gate voltage (V_F) and of the substrate back-gate voltage (V_B). The conductance modulation, indicated by the arrows, was observed in transistors containing a single boron atom [Figs. 1(b) and (c)] but not in an undoped one [Fig. 1(a)]. These modulations are due to the trapping of a single hole by the boron atom. From the capacitance analysis of the data, we have identified the depth position of the single boron atom as near the front interface (b) and around the middle of the silicon layer (c).

By doing similar analysis using drain bias as a parameter, we will also be able to obtain information about the dopant's lateral position, i.e., the position along the transport channel, which will lead us to a complete identification of dopant locations in a nanotransistor.

[1] Y. Ono et al., Appl. Phys. Lett. **90** (2007) 102106.

[2] M. A. H. Khalafalla et al., Appl. Phys. Lett. **91** (2007) 263513.

[3] Y. Ono et al., Appl. Surf. Sci. **254** (2008) 6252.

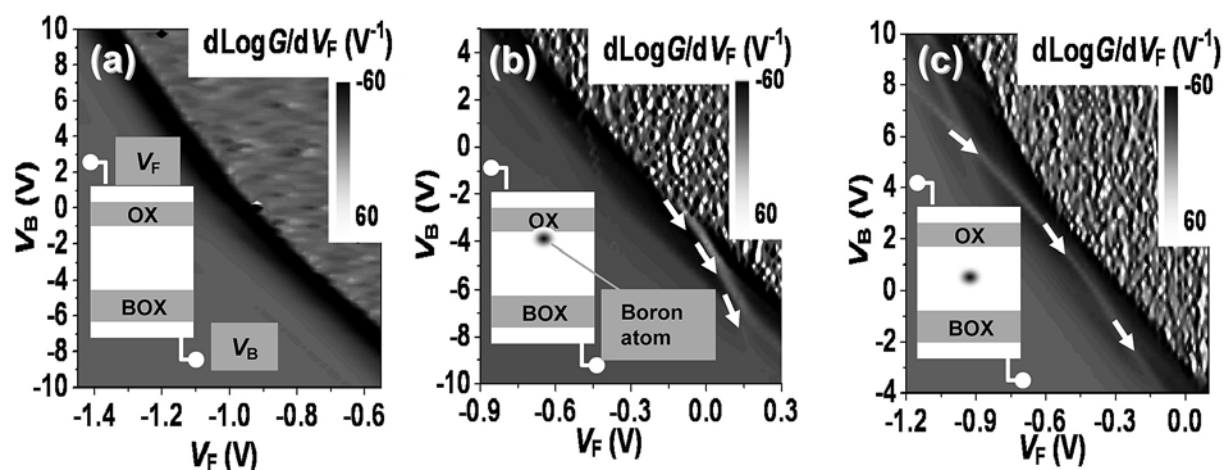


Fig. 1. Measurement results for an undoped transistor (a), and for transistors containing a single boron atom near the front-gate interface (b) and around the mid of the silicon layer (c). OX and BOX are the gate oxides of the front and back gates, respectively.

Bit Operation in a Parametrically Pumped Electromechanical Resonator

Imran Mahboob and Hiroshi Yamaguchi
Physical Science Laboratory

More than 150 years ago Charles Babbage originated the idea of a programmable computer. Babbage conceived his analytical engine in a mechanical architecture where logic was performed by moving parts. In the microelectronics age these ground breaking ideas were forgotten as silicon transistor technology was the system of choice for implementing logic. We demonstrate that in the era of nanotechnology the mechanical computer can be revived and logic can be implemented by electromechanical systems.

The Parametron is a logic processing system first developed 50 years ago [1]. It utilizes the parametrically excited resonance of a harmonic oscillator, where this oscillation has two stable phases separated by π radians, as the basis for logic operations. The computational architecture based on this principle was well developed using LC oscillators but was rendered obsolete by the transistor due to its high power consumption and integration difficulties in dense system architectures. To remedy these drawbacks, we propose to implement mechanical logic in the mould of the Parametron with electromechanical systems.

In the first steps to this goal, we demonstrate both bit storage and bit flip operations in an electromechanical oscillator [2]. We do this by integrating a two dimensional electron system into the mechanical oscillator which enables electromechanical transduction via the piezoelectric effect [3]. This enables on-chip all electrical actuation of the parametric resonance and detection of the fundamental mode as well as switching between the two phases of oscillation i.e. all the necessary prerequisites for the electromechanical Parametron computer. The electromechanical bit operation demonstrated here paves the way for realizing a nanomechanical computer.

[1] E. Goto, Proc. IRE **47** (1959) 1304.

[2] I. Mahboob and H. Yamaguchi, Nature Nanotechnol. **3** (2008) 275.

[3] I. Mahboob and H. Yamaguchi, Appl. Phys. Lett. **92** (2008) 173109.

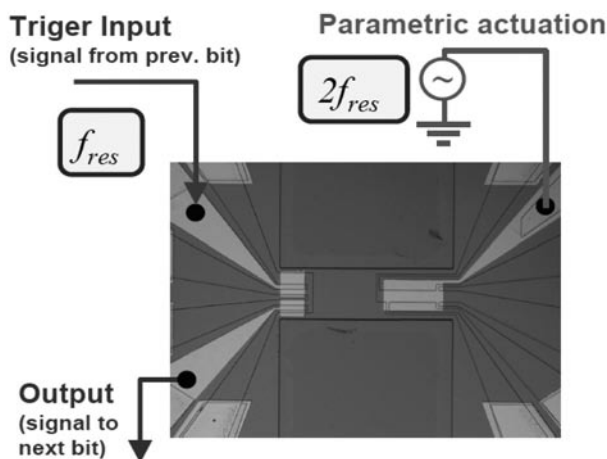


Fig.1. A microscope image of the electromechanical resonator integrating a two dimensional electron system, multiple Schottky contacted gold electrodes and a simplified circuit diagram which enabled the bit-flip operation to be implemented.

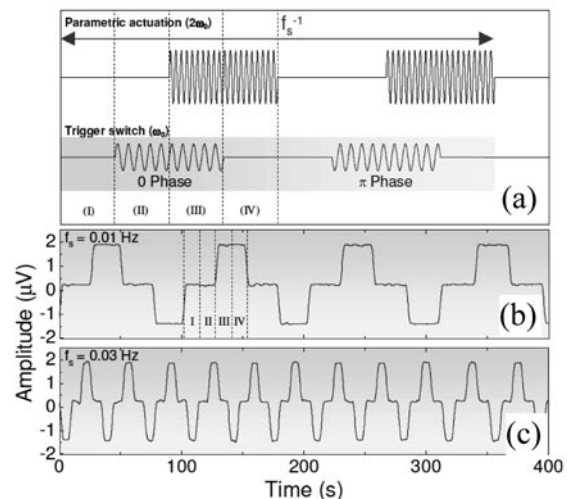


Fig.2. (a): a schematic of the pulse sequence at frequency f_s which enables bit storage and bit flip operations. (b) and (c): Experimental realization of the protocol described in (a) with $f_s=0.01$ and 0.03 Hz.

In-plane Conductance Measurements of Few-Layer Graphene on SiC Substrate

Masao Nagase, Hiroki Hibino*, Hiroyuki Kageshima, and Hiroshi Yamaguchi
Physical Science Laboratory, *Materials Science Laboratory

Graphene has recently attracted much attention due to its superior electric properties. Epitaxial graphene grown on SiC substrate is a promising material for beyond CMOS era because of its compatibility with existing wafer-scale manufacturing. Recently, a thickness determination method using low-energy electron microscopy (LEEM) with nanometer resolution has been established [1]. This technique enables us to control the layer number and morphology of few-layer graphene. The next challenge toward carbon based single-layer electronics using few-layer graphene is the characterization of local electric properties in order to evaluate the quality of grown graphene layers. We have developed several types of nanotools integrated on the Si cantilever of a scanning probe microscope (SPM) for measuring of the electrical properties of nanomaterials [2]. Here, we discuss local conductance images of few-layer graphene measured using our integrated nanogap probe with nanometer resolution [3].

Figure 1 show an in-plane conductance image of graphene nano-islands. The coverage of graphene is carefully controlled by LEEM observation to make the graphene nano-islands. The conductance measurement reveals the islands consist of single- and double-layer graphene. The measurement with this nanotool enables us to measure electrical properties of nanostructures on insulative substrate without the need for fabrication processes including lithography. Figure 2 is an in-plane conductance image of double-layer graphene grown on SiC substrate. It was confirmed by LEEM that the domain size of the single-crystal double-layer graphene is larger than terrace width of SiC substrate and up to few micrometers. As shown in Fig. 2, the local conductance of graphene is strongly affected by the surface morphology of the SiC substrate. Notably, an atomic layer step buried under the graphene layer remarkably reduces the conductance of graphene. The conductance mapping with nanometer resolution will be helpful in developing carbon-based single-layer electronics.

This work was partly supported by KAKENHI (19310085, 20246064).

- [1] H. Hibino et al., Phys. Rev. B **77** (2008) 075413.
- [2] M. Nagase et al., Jpn. J. Appl. Phys. **46** (2007) 5639.
- [3] M. Nagase et al., Nanotechnol. **19** (2008) 495701.

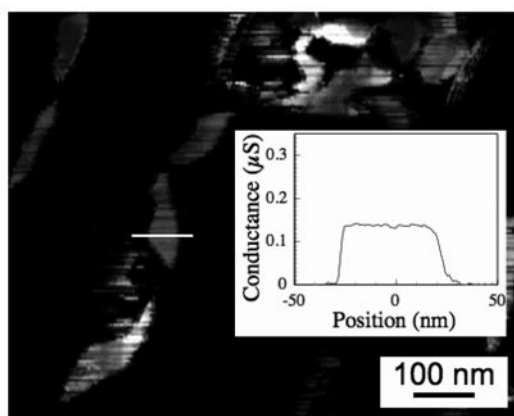


Fig. 1. In-plane conductance image of graphene nano-islands on SiC substrate. Inset is a conductance profile of an individual nanoisland.

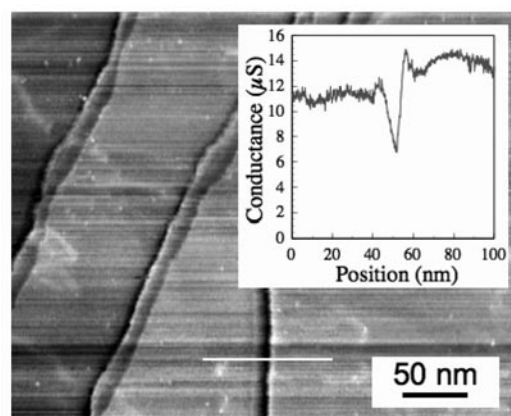


Fig. 2. In-plane conductance image of double-layer graphene measured using integrated nanogap probe. Inset is a conductance profile at an atomic layer step.

Fabrication of Three-Dimensional Nanostructures by Electron Beam Lithography

Kenji Yamazaki and Hiroshi Yamaguchi
Physical Science Laboratory

Three-dimensional (3D) nanostructures are now attracting great interest because of their possible applications, such as to nanomechanical devices and nanorobotics. To build various 3D nanostructures, we have devised and are developing 3D electron beam (EB) lithography (3D-EBL). Although our technique has some advantages, such as high resolution and fast fabrication, it has so far shown drawbacks related to the electron scattering/proximity effect and to the poor precision of structure/3D alignment, compared with some other 3D fabrication techniques. We have newly devised two methods in 3D-EBL to significantly improve the 3D alignment and reduce the proximity effect.

When we make complicated 3D structures with this technique, the EB writes from largely different directions and therefore should be well positioned three-dimensionally; high accuracy of 3D alignment is necessary. The high accuracy is achieved by using a transmission electron image to accurately control sample rotation (< 1 mrad) and obtain sufficient accuracy of 2D positioning of EB writing on a rotated sample [1]. In a 3D nanostructure we created in negative resist (hydrogen silsesquioxane, HSQ), the 3D alignment accuracy is on the order of 10 nm (Fig. 1). When we use positive resist, the proximity effect is very serious. However, we have succeeded in suppressing the proximity effect by leaving buffer areas (not exposed to EB) that surround the target structure and have sizes similar to the range of fast secondary electrons. As a result, we have reduced undesirable dissipated energy, which changes vertically in the resist [2]. Figure 2 shows SEM images of a 3D nanostructure in positive resist [poly(methyl methacrylate), PMMA], which demonstrates a high aspect ratio and the great flexibility of structures that can be created by the technique.

These methods will accelerate the development of 3D-EBL, making it promising for various nanotechnology applications.

This work was supported in part by KAKENHI (20246064).

[1] K. Yamazaki and H. Yamaguchi, *J. Vac. Sci. Technol. B* **26** (2008) 2529.

[2] K. Yamazaki and H. Yamaguchi, *Appl. Phys. Exp.* **1** (2008) 098001.

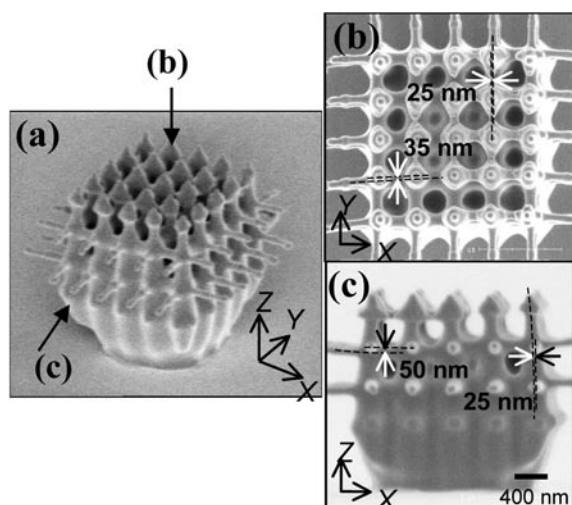


Fig. 1. 3D nanostructure in HSQ, made by writing arrays of dots from $\pm X$, $\pm Y$, and Z directions.

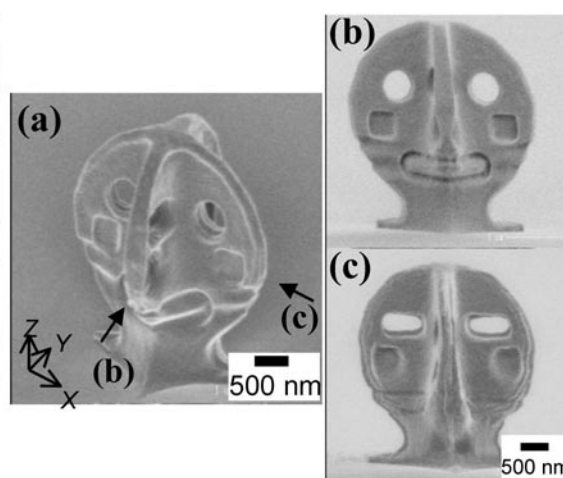


Fig. 2. 3D nanostructure in PMMA, made by leaving buffer areas to suppress the proximity effect.

Direct Measurement of the Binding Energy and Bohr Radius of a Single Hydrogenic Defect in a Semiconductor Quantum Well

Simon Perraud, Kiyoshi Kanisawa, Zhao-Zhong Wang, and Toshimasa Fujisawa
Physical Science Laboratory

Impurities are fundamentally important for semiconductor device fabrication. In the simplest approximation, an impurity, or a point defect, inside a semiconductor is described as a hydrogen atom. The two essential properties of such impurity are the binding energy and the Bohr radius (a_{B1}). Impurities in quantum wells (QWs) are affected by the confining potential if $a_{B1} \geq l$, where l is the QW thickness. (111)A-oriented, nominally undoped $\text{In}_{0.53}\text{Ga}_{0.47}\text{As}$ surface QWs were grown by molecular beam epitaxy (MBE) [1]. We used the scanning tunneling microscope (STM) and the spectroscopy (STS) at the low-temperature (5 K) to study point defects behaving like donor impurities, which are natively located at the epitaxial surface of a QW. The electronic local density of states (LDOS) was measured with nanoscale resolution in the vicinity of single point defects. By measuring the LDOS in the QW, we are able to determine both the binding energy and the Bohr radius of single defects. Four different QW thicknesses were investigated in this work ($l=2, 6, 10,$ and 14 nm). The obtained spatial dependence as the function of the distance r is well fitted by an exponential decay proportional to $\exp(-2r/a_{B1})$, representing the $1s$ hydrogenic wave function. Figure 1 summarizes the STS data obtained in this work. The smaller l , the larger binding energy $E_1 - \varepsilon_1$, and the smaller a_{B1} , i.e. the tighter the electron is bound to the point defect. Here, E_1 is the bottom of the two-dimensional subband of the QW, and ε_1 is the ground level of the impurity bound states. We clearly observe the influence of quantum confinement on the bound states, as expected in the case $a_{B1} \geq l$. If STS data are compared with a calculation of hydrogenic impurity states, the binding energy and the Bohr radius were found to be functions of the quantum well thickness, in quantitative agreement with variational calculations of hydrogenic impurity states [2]. It is remarkable that this calculation requires no adjustable parameter. The increase of $E_1 - \varepsilon_1$ (or, equivalently, the decrease of a_{B1}) with decreasing l is enhanced by the conduction band nonparabolicity.

- [1] S. Perraud, K. Kanisawa, Z.-Z. Wang, and T. Fujisawa, *Phys. Rev. B* **76** (2007) 195333.
[2] G. Bastard, *Phys. Rev. B* **24** (1981) 4714.

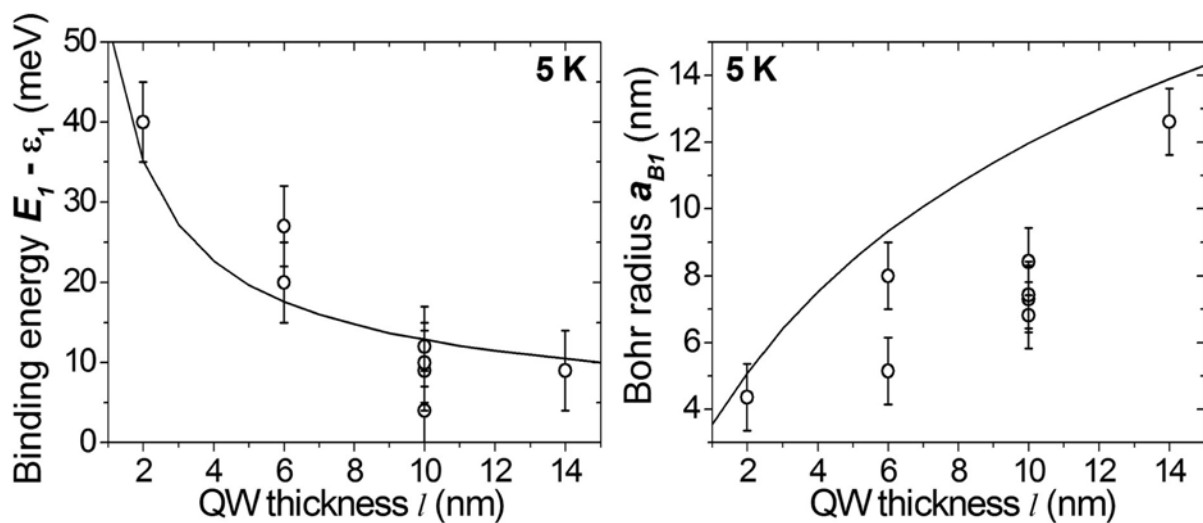


Fig. 1. Binding energy $E_1 - \varepsilon_1$ and Bohr radius a_{B1} as a function of QW thickness l : STS data (each circle corresponds to a single point defect at the $\text{In}_{0.53}\text{Ga}_{0.47}\text{As}$ QW surface), and hydrogenic model (solid curves).

Electrons and Holes in a Single Silicon Slab

Kei Takashina and Koji Muraki
Physical Science Laboratory

Electron-hole bilayers in which a two-dimensional electron gas (2DEG) and a two-dimensional hole gas (2DHG) coexist in close proximity have received considerable interest owing to the possibility of their hosting a condensation of indirect dipolar excitons [1]. Here, we examine the low temperature transport properties of a device in which electrons and holes are simultaneously generated but separately contacted [2] in a 40 nm thick layer of silicon.

The device consists of a Silicon-On-Insulator transistor [Fig. 1(a)] in which the front- and back-gates allow sufficient electric field in the silicon quantum well to overcome the band-gap so that a 2DEG and 2DHG can be generated simultaneously at opposite sides of the well. The device is cut into a Hall-bar where each of the arms is terminated by *p*- and *n*-type contacts [Fig. 1(b)] made by ion implantation of B and P respectively [3]. The *n*-contacts (*p*-contacts) connect to the 2DEG (2DHG) but the *p*-contacts (*n*-contacts) do not due to the depletion regions formed at each junction between the 2DEG (2DHG) and the *p*-contacts (*n*-contacts) leading to independent contacts.

Low temperature measurements of Shubnikov de Haas oscillations [Fig. 1(d) and Fig. 1(e)] show that the charge carriers are generated at the expected positions in the structure [Fig. 1(c)] and that their densities can be controlled by an interlayer bias applied between the 2DEG and 2DHG in addition to the gate voltages. This allows the electric field (confinement potential) to be tuned in the quantum well, and in turn allows the physical properties of the carriers such as the strength of disorder and electronic valley splitting to be controlled [4]. We confirm that drag measurements are possible with the structure [5]. We expect that the structure will allow many new measurements to probe the physics of electron-hole systems.

- [1] Y. E. Lozovik and V. I. Yudson, JETP Lett. **22** (1975) 556.
 [2] U. Sivan, P. M. Solomon, and H. Shtrikman, Phys. Rev. Lett. **68** (1992) 1196.
 [3] K. Takashina et al., Extended Abstracts of the 2006 International Conference on Solid State Devices and Materials, Yokohama 2006, pp.830-831; K. Takashina et al., Jpn. J. Appl. Phys. **46** (2007) 2596; M. Prunnila et al., Appl. Phys. Lett. **93** (2008) 112113.
 [4] K. Takashina et al., Phys. Rev. Lett. **96** (2006) 236801.
 [5] K. Takashina et al., Appl. Phys. Lett. **94** (2009) 142104.

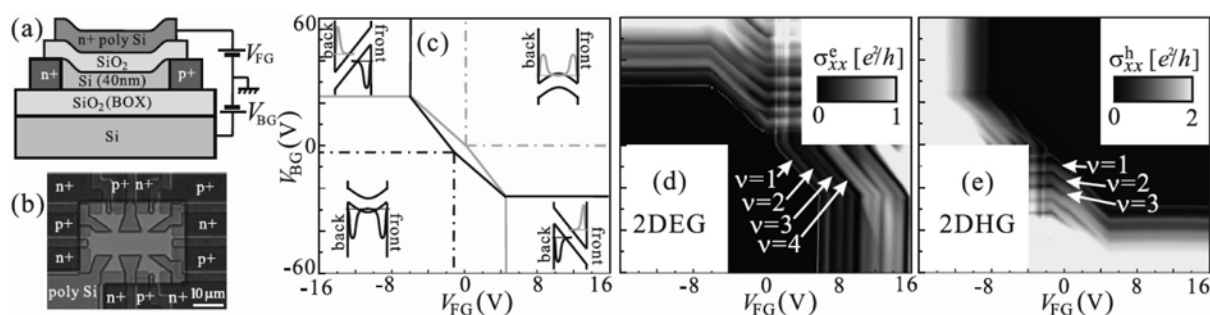


Fig. 1. (a) A schematic diagram of the device. (b) An optical micrograph of a Hall bar. The voltage probes are terminated by *n*- and *p*-type contacts. (c) Schematics of the confinement potential in different regions of (V_{FG} , V_{BG}) for data shown in (d) and (e). (d) and (e) show conductivity at $B=15$ T, $T\sim 250$ mK taken using *n*- and *p*-type contacts respectively with an interlayer bias voltage of 0.6 V.

New Readout Method for Josephson Persistent-Current Qubits Using a Josephson Bifurcation Amplifier

Kosuke Kakuyanagi, Seiichiro Kagei*, Ryota Koibuchi*, and Kouichi Semba
Physical Science Laboratory, *Tokyo University of Science

A superconducting flux qubit has potential for use as a device in quantum computing. To read the qubit state, we usually use a SQUID to detect the small magnetic field generated by the supercurrent of a superconducting flux qubit [1]. However, this readout method changes the SQUID state to the voltage state, so the backaction of the measurement is large and high-speed measurement is also difficult. This makes it hard to execute the quantum algorithm, which reads the qubit state several times during the coherence time. Therefore, we attempt to read flux qubits using a Josephson bifurcation amplifier (JBA) [2], which employs the bistability of a non-linear resonance circuit. With this readout method, the Josephson junction superconducting state is maintained during the measurement thus making it possible to achieve a fast and ultimately small backaction readout as with a quantum non-demolition measurement.

We design the flux qubit and SQUID structure at the center of a coplanar waveguide, both sides of which are connected to a capacitor. We then measure the transmission characteristics of this sample. Because of the non-linearity of the Josephson junction, the resonance frequency shifts to the lower frequency side with increases in applied microwave power, and the resonance spectrum shows a jump above the critical microwave power. This is a transition from one stable state to another and means that the bistable state of the non-linear resonator has appeared. The stable resonance state that appears depends on the resonator state. So, by realizing magnetic coupling between a nonlinear resonator and a qubit, we can reflect the flux qubit state to the resonator and read the qubit state. We can measure the qubit state by the homodyne detection of a transmission microwave because the amplitude and phase of the transmission microwaves of each stable resonance state are different. Then we attempt to read the qubit state by employing pulsed microwaves. Figure 1 shows a block diagram of a pulse measurement system and an example readout. A pulse-modulated microwave passes through the JBA circuit and is amplified. The signal interferes with the reference microwave, and then we can obtain 0-degree and 90-degree phase components. From this amplitude and phase information, we can clearly separate two states and successfully read the flux qubit state [3].

This work was supported by KAKENHI(18201018,18001002).

[1] Caspar H. van der Wal et al., *Science* **290** (2000) 773.

[2] I. Siddiqi et al., *Phys. Rev. Lett.* **93** (2004) 207002.

[3] K. Semba, K. Kakuyanagi et al., *Quantum Information Processing* **8** (2009) 199.

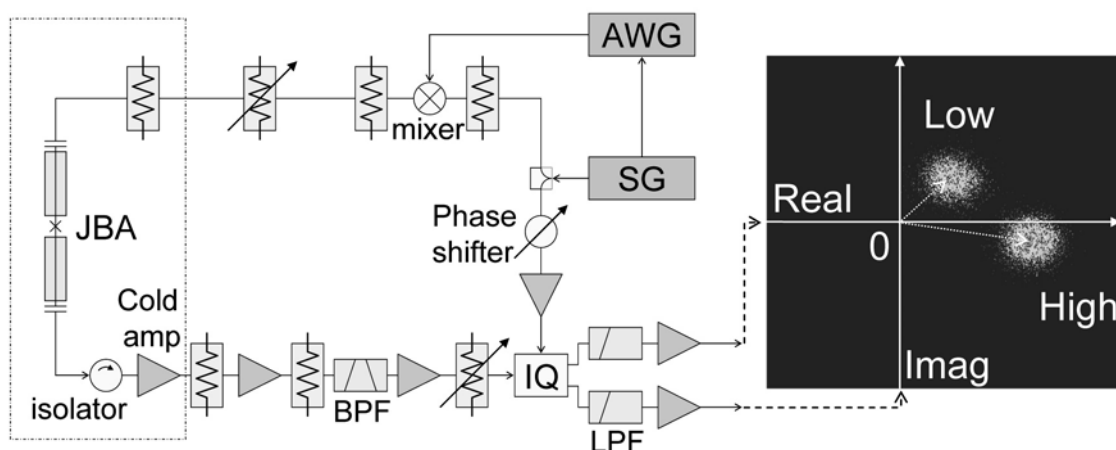


Fig.1. Block diagram of JBA pulse readout (left) and result of qubit state readout (right).

Evidence of Noise-Suppression with Superconductive Atom Chip

Tetsuya Mukai, Christoph Hufnagel, and Fujio Shimizu*
Physical Science Laboratory

*The University of Electro-Communications / NTT Research Professor

Strong confinement in trapping neutral atoms is necessary to realize full quantum control over atomic system. Although micro-magnetic trap on chip is a promising candidate to realize a strong trapping confinement, the electro-magnetic noise and thermal noise reduce the trapping lifetime seriously in the vicinity of a chip surface. To overcome this problem we developed a persistent supercurrent atom chip [1], and in 2008 we have shown an evidence of noise-suppression of superconductive atom chip even in the vicinity of a strip with large transporting current.

The experiment was done by measuring the number of atoms leftover after keeping atoms in a chip potential with specific atom-surface distance. An absorption measurement with reflected image was employed for precise trap height identification (Fig. 1). The chip pattern that we used for this experiment has an MgB_2 superconductive loop circuit as shown in Fig. 2. Figure 3 represents the measured trapping lifetime over the atom-surface distance, which was deduced from the decay late of trapped atoms. The lifetime of our persistent supercurrent atom chip was reaching more than an order longer than that of normal conductive counterparts. With miniaturized wire strip, we will realize a strong trapping confinement in quantum regime, and in future we will pursue the realization of full quantum control over atomic system.

This research was partially supported by Japan Science and Technology Agency CREST.

[1] T. Mukai, C. Hufnagel et al., Phys. Rev. Lett. **98** (2007) 260407.

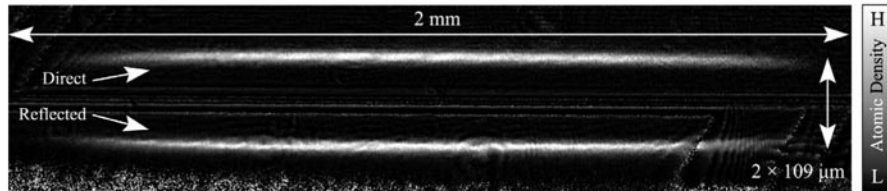


Fig. 1. Sample absorption image of trapped atomic cloud with reflection in the vicinity of a chip surface.

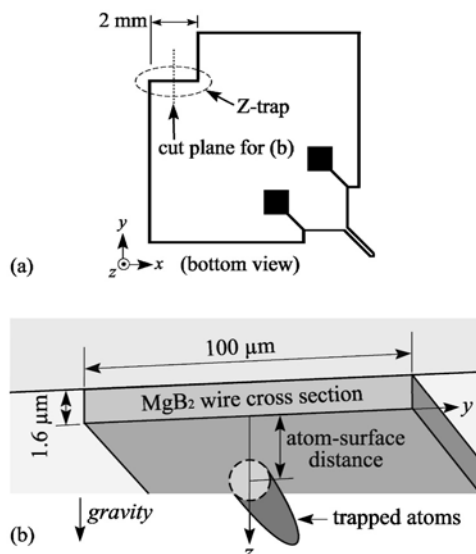


Fig. 2. (a) Chip pattern of persistent supercurrent atom chip. (b) Cross section of the chip wire and the trap geometry.

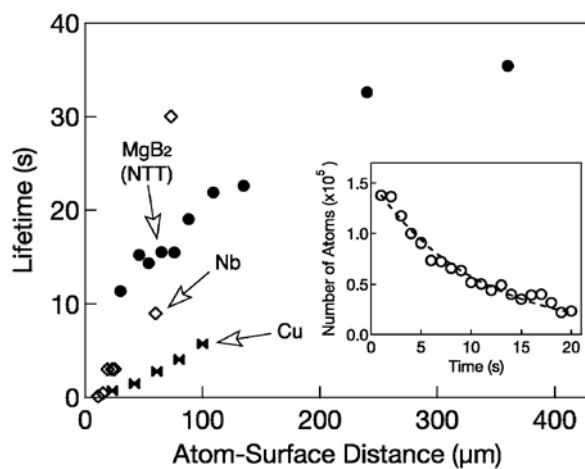


Fig. 3. Trapping lifetime over the atom-surface distance. (Ref: Eur. Phys. J. D **51** (2009) 173 and Phys. Rev. A **66** (2002) 041604.)

Single-Shot Readout of a Josephson Persistent Current Quantum Bit

Kouichi Semba, Hiroataka Tanaka, Shiro Saito, and Hayato Nakano
Physical Science Laboratory

In order to measure the quantum state of a persistent current quantum bit (a flux qubit), we use a dc-SQUID as a detector [1]. By carefully designing the junction parameters, the inner loop of Fig. 1(a) can be made to behave as an effective quantum two-state system, qubit. The qubit is described by the Hamiltonian $H_q = (\epsilon_f \sigma_z + \Delta \sigma_x) / 2$, where $\sigma_{x,z}$ are the Pauli matrices. Due to the fluxoid quantization, the two eigenstates of σ_z are almost localized states with the supercurrent circulating in opposite directions, i.e., the clockwise state $|R\rangle$ and the counter-clockwise state $|L\rangle$. The dc-SQUID picks up a signal that is proportional to σ_z . Figure 2(a) shows the modulation of the measured dc-SQUID switching current against the external magnetic flux as a function of $f = \Phi_{\text{ext}} / \Phi_0$, where Φ_0 is a flux quantum $h/2e$. Each dot in the graph corresponds to every single readout without averaging. The classically stable current eigenstates $|L\rangle$ and $|R\rangle$ are no longer stable in the presence of quantum tunneling Δ . As shown in Fig. 2(b), qubit energy eigenstates $|0\rangle$ and $|1\rangle$ are superpositions of macroscopically distinct states $|L\rangle$ and $|R\rangle$. In Fig. 2(e) near $f=1.5$, where $\Delta \gg \epsilon_f \sim 0$ and the switching current distribution is sharp enough to observe the χ -shaped qubit step clearly. The thicker stripe corresponds to the ground state $|0\rangle$ and the other stripe corresponds to the excited state $|1\rangle$. These facts clearly show that we can carry out a single-shot σ_z projection measurement to $|L\rangle$ or $|R\rangle$ with the aid of a Φ_{ext} shift pulse, in the same way as the Stern-Gerlach apparatus for measuring a superposed spin-state. The merit of our dc-SQUID readout is that we can control interaction strength between the qubit and the detector dc-SQUID, at will. In the Stern-Gerlach case, it was always fixed and was definitely larger than energy difference of the spin eigenstates. This gives us a possibility of realtime control of the quantum readout itself.

[1] K. Semba et al., Quantum Information Processing **8** (2009) 199.

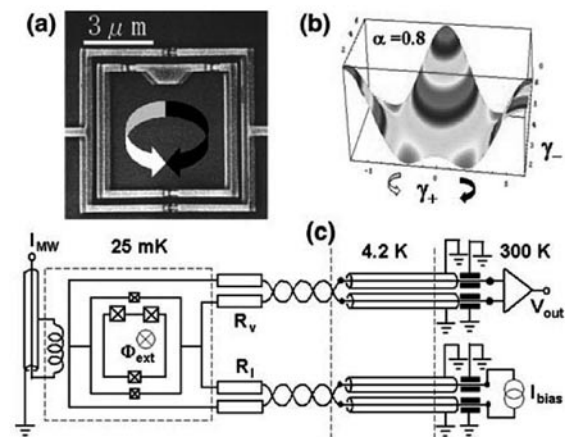


Fig. 1. (a) Scanning electron micrograph of a superconducting qubit (inside loop) and a dc-SQUID (outside loop) as a detector. A pair of arrows indicate distinct supercurrent states $|L\rangle$ and $|R\rangle$ of the qubit. (b) The potential energy of the qubit in phase space. (c) Schematic diagram of the measurement setup. Qubit was measured at dilution temperature of 25 mK.

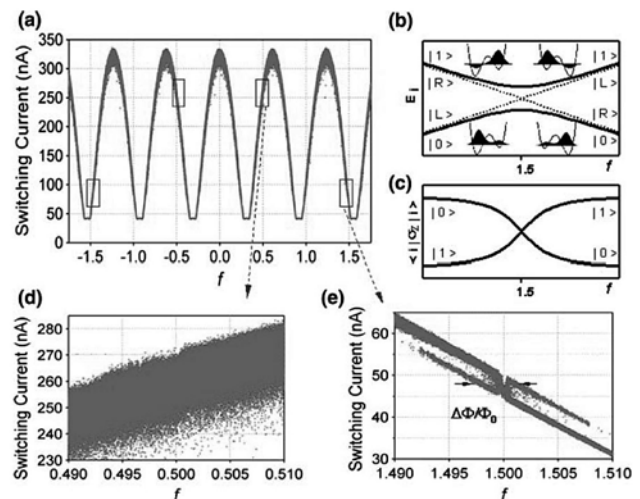


Fig. 2. (a) Switching current of the dc-SQUID detector. $f = \Phi_{\text{ext}} / \Phi_0$, where Φ_{ext} is the external magnetic flux penetrating the qubit loop. (b) Schematics of the qubit energy eigenstates $\{|0\rangle, |1\rangle\}$ and current eigenstates $\{|L\rangle, |R\rangle\}$. (c) Expected readout for states $\{|0\rangle, |1\rangle\}$. (d) Zoom in near $f=0.5$. (e) Zoom in near $f=1.5$. Qubit states $|0\rangle$ and $|1\rangle$ can be readout distinctly.

Photoluminescence Spectroscopy of Nonlinear- and Linear-Screening Regimes in a Low-Density Two-Dimensional Electron System

Masumi Yamaguchi¹, Shintaro Nomura², Yoshiro Hirayama³,
Hiroyuki Tamura¹, and Tatsushi Akazaki¹

¹Physical Science Laboratory,
²University of Tsukuba/NTT Research Professor, ³Tohoku University

A high-quality low-density two-dimensional electron system (2DES) in semiconductors can be formed on gated undoped GaAs quantum wells (QWs) grown by molecular beam epitaxy. Some interesting phenomena, such as Wigner crystallization, are predicted to appear in low-density 2DES theoretically because the large Coulomb interaction between electrons plays a role. However, the unavoidable potential randomness in real samples disturbs the ideal 2D condition. Investigating the screening of the potential randomness by the induced electrons would therefore help us to better understand the low-density 2DES properties.

In this study, we performed photoluminescence (PL) measurements on an undoped GaAs QW for different electron densities with a gate bias. We found a two-stage transition reflecting the change of the potential-screening properties when the electrons were induced [1]. By PL measurement, we can seamlessly follow the transition from the insulating to the metallic regimes through the PL spectrum change from the exciton (X_0) and charged exciton (X^-) to the 2DES-hole recombination. The typical PL spectra are shown in Fig. 1 from the bottom to top with increasing gate bias voltage. The two-stage change of PL intensity and linewidth against the gate bias voltage, shown in Fig. 2, corresponds to the transition from the electron localization in the insulating regime to the linear screening in the metallic regime through a non-linear screening regime. In the linear screening regime, the induced electrons effectively screen the random potential, whereas the electrons partially screen the random potential valley in the non-linear screening regime. The randomness of our sample may originate from electrons trapped in the surface state. A sample with a larger distance from the surface to the QW may reduce the random potential at low electron density.

This work was partly supported by CREST program of Japan Science Technology Agency.

[1] M. Yamaguchi et al., Phys. Rev. Lett. **100** (2008) 207401.

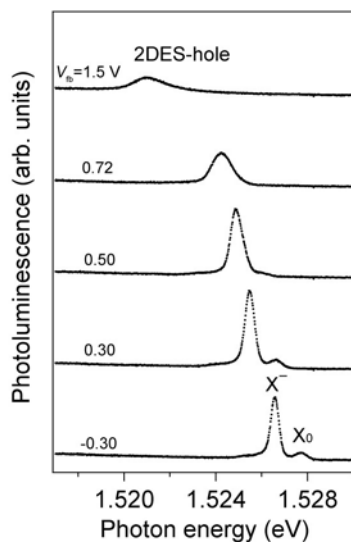


Fig. 1. Photoluminescence spectra for different gate bias voltages.

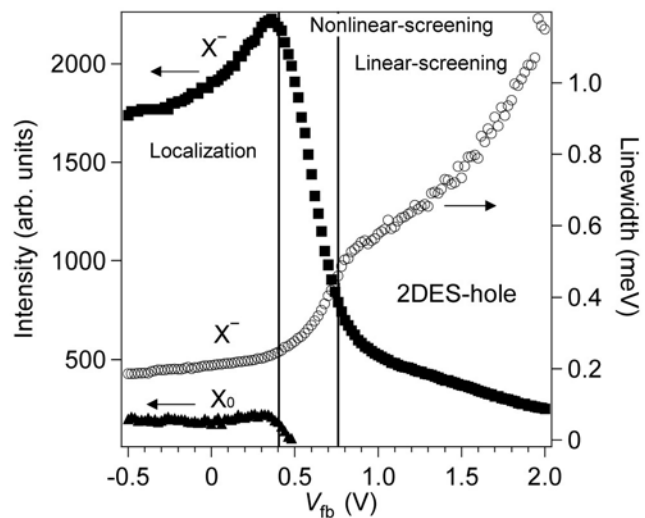


Fig. 2. Photoluminescence intensity and linewidth against the bias voltage.

Negative Photoconductivity in $\text{In}_{0.52}\text{Al}_{0.48}\text{As}/\text{In}_{0.7}\text{Ga}_{0.3}\text{As}$ Heterostructures

Tatsushi Akazaki¹, Masumi Yamaguchi¹, Kohei Tsumura²,
Shintaro Nomura³, and Hideaki Takayanagi⁴

¹Physical Science Laboratory, ²University of Tsukuba,

³University of Tsukuba/NTT Research Professor, ⁴Tokyo University of Science

InGaAs-based heterostructures with a large Rashba spin-orbit interaction are very attractive for applications in semiconductor spintronics [1]. In terms of spin manipulation, it is very important to investigate the optical effect on the transport properties in these InGaAs-based heterostructures. This is because spin-aligned carriers are generated when electrons are excited by circularly polarized light. In this study, we investigated the transport of a two-dimensional electron gas (2DEG) in an $\text{In}_{0.52}\text{Al}_{0.48}\text{As}/\text{In}_{0.7}\text{Ga}_{0.3}\text{As}$ heterostructure when exposed to light from infrared laser diodes ($\lambda=0.78, 1.3 \mu\text{m}$) [2].

In the dark, the sheet carrier density n_{Hall} and mobility μ of the 2DEG at 1.8 K obtained with Hall-effect measurements were found to be $\sim 2.3 \times 10^{12} \text{ cm}^{-2}$ and $\sim 161,000 \text{ cm}^2/\text{Vs}$, respectively. To investigate the optical effect, the laser light was guided through an optical fiber close to the surface of a Hall-bar sample placed in a magnetic field of 0.5 T at 1.8 K. The Hall voltage was measured before, during and after illumination. The n_{Hall} was estimated using the measured Hall voltage. Figure 1 shows the time dependence of n_{Hall} before, during and after illumination with (a) 1.3 μm and (b) 0.78 μm light. When the sample was illuminated with 1.3 μm light, n_{Hall} immediately decreased and became constant, although photo-induced carriers were generated in the $\text{In}_{0.7}\text{Ga}_{0.3}\text{As}$ channel layer. After the illumination was switched off, n_{Hall} slowly increased and regained its initial value after about one hour. In contrast, when the sample was illuminated with 0.78 μm light, n_{Hall} increased slightly only during illumination. We concluded that negative photoconductivity occurs in $\text{In}_{0.52}\text{Al}_{0.48}\text{As}/\text{In}_{0.7}\text{Ga}_{0.3}\text{As}$ heterostructures when they are illuminated by photons with $\lambda=1.3 \mu\text{m}$, namely at the longer wavelength (lower energy), in contrast to several previous reports stating that negative photoconductivity in InAs/AlSb heterostructures occurs only when they are illuminated by photons with a relatively high energy [3]. We would speculate that the negative photoconductivity in $\text{In}_{0.52}\text{Al}_{0.48}\text{As}/\text{In}_{0.7}\text{Ga}_{0.3}\text{As}$ heterostructures is attributed to the presence of the deep impurity levels in the $\text{In}_{0.52}\text{Al}_{0.48}\text{As}$ layer.

This work was partly supported by CREST program of Japan Science Technology Agency.

[1] J. Nitta et al., Phys. Rev. Lett. **78** (1997) 1335.

[2] T. Akazaki et al., Physica E **40** (2008) 1341.

[3] Yu. G. Sadofyev et al., Appl. Phys. Lett. **86** (2005) 192109.

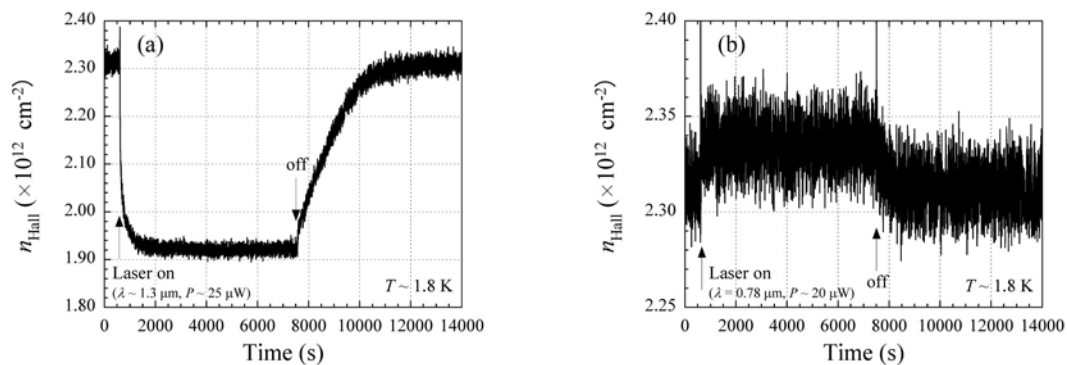


Fig. 1. Time dependence of sheet carrier density n_{Hall} at 1.8 K before, during and after illumination with (a) 1.3 μm and (b) 0.78 μm light.

Numerical Simulation of Ultracold Atoms Trapped in Optical Lattices

Makoto Yamashita
Optical Science Laboratory

Ultracold atoms have been stimulating many researchers' interest after a successful realization of Bose-Einstein condensation in 1995. Recent noteworthy progress on atom manipulation techniques has led to unprecedented experiments demonstrating an extremely high controllability. An optical lattice, formed by a standing wave of counter-propagating laser lights as shown in Fig. 1, is a typical example that allows us to investigate fundamental quantum many-body problems found in condensed matter physics via atomic gases.

We have developed a highly efficient numerical method based on the Gutzwiller approximation and analyzed the ground state properties of ultracold atoms trapped in optical lattices [1]. To examine the quantitative ability of our method, we numerically simulated the recent experiment performed by MIT group [2] which precisely observed the quantum phase transition of bosonic atoms in a three-dimensional optical lattice. Figure 2(a) shows the average number distribution of atoms over the lattice sites in the $y=0$ plane for the superfluid phase where the depth of optical lattice is relatively shallow. Note that 560,000 lattice sites and 300,000 atoms are assumed in our calculations. The smooth and convex atom distribution is obtained reflecting a weak magnetic confining potential in the experiment. Figure 2(b), on the other hand, shows the number distribution for the Mott-insulator phase where the lattice depth is deep enough. Due to the strong repulsive interactions between the atoms, the average number takes the discrete values ranging from $n=1$ to $n=5$, which leads to a stepwise distribution. From this result, we understand that ultracold atoms in the Mott-insulator phase form an intriguing shell structure in their spatial distribution. The calculated results in Fig. 2 agree well with the experimental observations of MIT group and we have confirmed an excellent quantitative performance of our numerical simulations.

This work was supported in part by Japan Science and Technology Agency, CREST.

- [1] M. Yamashita and M. W. Jack, Phys. Rev. A **79** (2009) 023609.
[2] G. K. Campbell et al., Science **313** (2006) 649.

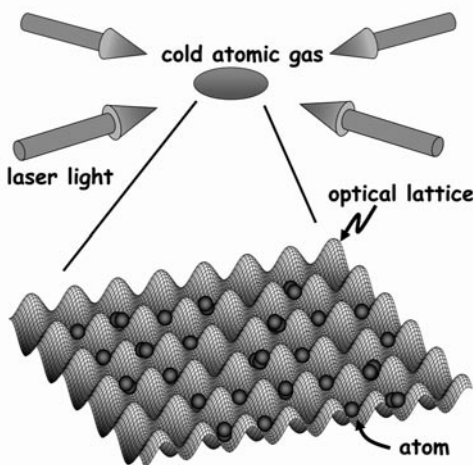


Fig. 1. Schematic diagram of ultracold atomic gas trapped in an optical lattice.

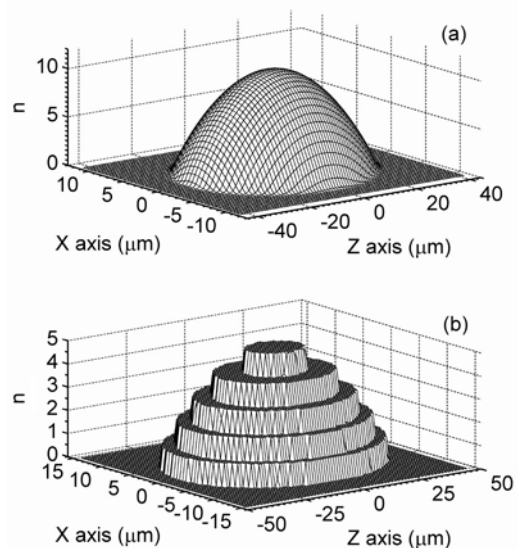


Fig. 2. Number distributions in the $y=0$ plane: (a) superfluid state and (b) Mott-insulator state.

Single Photon Detection Using MgB₂ Superconductor

Hiroyuki Shibata
Optical Science Laboratory

Quantum cryptography is the ideal way to achieve secure communications, since the security is guaranteed by the physical principle of quantum mechanics. To realize a quantum cryptography network, it is necessary to strongly increase the communications distance and speed, which are limited by the performance of conventional single photon detectors. Recently, a new type of single photon detector that uses NbN superconducting nanowire (SSPD) has been developed. In quantum key distribution (QKD) experiments, NbN-SSPD has substantially outperformed conventional semiconducting single photon detectors [1]. Here, we are investigating single photon detection using MgB₂ superconductor. Since T_c of MgB₂ is 40 K, which is much higher than the 16 K of NbN, a MgB₂-SSPD would have a higher operating temperature. Moreover, the short electron-phonon relaxation time of MgB₂ means that the MgB₂-SSPD would operate faster than a NbN-SSPD.

To fabricate the MgB₂-SSPD, it is necessary to develop a technique for MgB₂ ultra-thin film growth and to develop a MgB₂ nano-fabrication process. We use the molecular-beam epitaxy (MBE) for the ultra-thin film growth, and have obtained the 10-nm-thick MgB₂ film with T_c of 20 K. For nano-fabrication of NbN, reactive ion etching (RIE) with fluorine-based gas has been established, but no etching gas has been reported for MgB₂. We have developed a new lift-off process using a Si/C bilayer mask, which can withstand the high temperatures needed for MgB₂ deposition. Using the method, we have fabricated a MgB₂ nanowire with a width of 200 nm. Figure 1 shows the MgB₂ nanowire, which is illuminated by a laser pulse from an optical fiber. When the nanowire is biased by a dc current source, electrical signals with a repetition frequency of 100 MHz appear, corresponding to the laser pulse [Fig. 2(a)]. The signals become intermittent as the intensity of the laser pulse strongly decreases [Fig. 2(b), (c)], indicating that the MgB₂ nanowire works in the photon detection regime [2].

[1] H. Takesue et al., *Nature Photon.* **1** (2007) 343.

[2] H. Shibata et al., *IEEE Trans. Appl. Supercond.* **19** (in press).

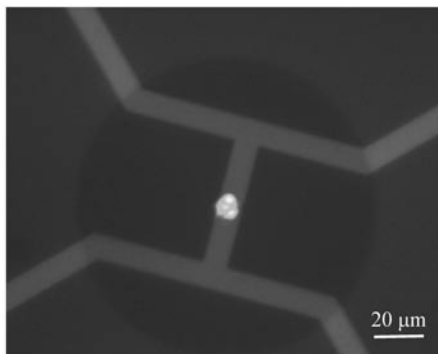


Fig. 1. Photograph of the MgB₂ nanowire photon detector illuminated by laser light from an optical fiber.

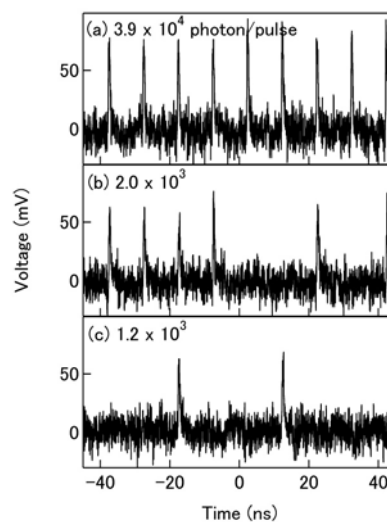


Fig. 2. Optical power dependence of output signals.

Generation of High-Purity Entangled Photon Pairs Using Silicon Wire Waveguide

Ken-ichi Harada, Hiroki Takesue, Hiroshi Fukuda*, Tai Tsuchizawa*,
Toshifumi Watanabe*, Koji Yamada*, Yasuhiro Tokura, and Sei-ichi Itabashi*
Optical Science Laboratory, *Microsystem Integration Laboratories

Recently, 1.5- μm band entangled photon pair generation using spontaneous four-wave mixing (SFWM) in a silicon wire waveguide (SWW) has been drawing attention [1]. An SWW is expected to function as a high-purity entangled photon pair generation device. By using an SWW, we obtained two-photon interference fringes of time-bin entangled photons with $> 95\%$ visibilities [2].

An SWW is a nano-scale silicon waveguide fabricated on silicon-on-insulator wafer [3]. An SWW exhibits very large third order nonlinearity because of its extremely small effective area, and thus we can obtain efficient SFWM in a waveguide whose length is ~ 1 cm.

Figure 1 shows experimental setup. The laser light is modulated into double pulses with a repetition frequency of 100 MHz by using an intensity modulator (IM). The pulse width and interval are 90 ps and 1 ns, respectively. The double pulses are input into an SWW. The SWW used in the experiment is 460 nm wide, 200 nm thick, and 1.15 cm long. The excess loss of the SWW is 1.0 dB. Consequently, time-bin entangled photon pairs are generated through the SFWM in the SWW. The photons from the SWW are launched into a fiber Bragg grating (FBG) to suppress the pump photons, and input into an arrayed waveguide grating (AWG) to separate the signal and idler photons. The signal and idler wavelengths are ± 3.2 nm from the pump wavelength. Each photon is then launched into a 1-bit delayed interferometer fabricated using planar lightwave circuits (PLC) based on silica waveguide technology. The phase difference between two paths of the interferometer is precisely controlled by adjusting the temperature of the substrate. The photons from the PLC interferometers are received by single photon detectors (SPD) operated in a gate mode whose gate frequency is 100 MHz.

We fixed the signal interferometer temperature and counted the coincidences while changing the idler interferometer temperature (fig. 2). The solid and dashed lines represent the measurement results obtained with nonorthogonal measurement bases for the signal photons. The visibilities of fitted curves are 96.3% (solid) and 95.2% (dashed). Thus, we successfully confirmed the generation of a high-purity entangled state in the 1.5- μm band.

[1] H. Takesue et al., *Appl. Phys. Lett.* **91** (2007) 201108.

[2] K. Harada et al., *Opt. Express* **16** (2008) 20368.

[3] T. Tsuchizawa et al., *IEEE J. Sel. Top. Quantum Electron.* **11** (2005) 232.

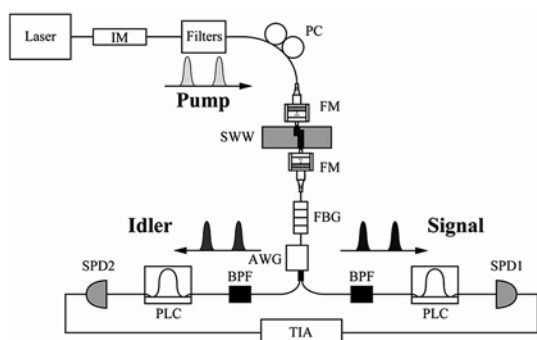


Fig. 1. Experimental setup. PC: polarization controller, FM: focusing module, BPF: band pass filter, TIA: time interval analyzer.

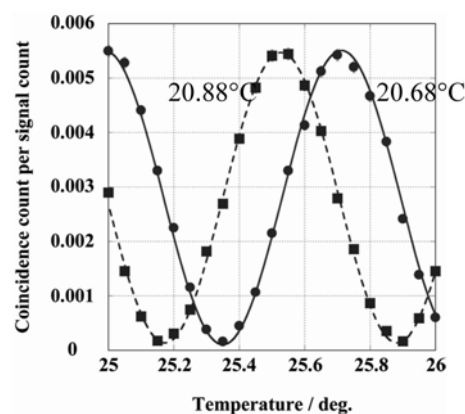


Fig. 2. Two-photon interference fringes.

Efficient Carrier Envelope Offset Locking for a Frequency Comb by Modifying a Collinear f -to- $2f$ Interferometer

Atsushi Ishizawa, Tadashi Nishikawa, and Hidetoshi Nakano
Optical Science Laboratory

The development of the mode-locked laser has contributed to our ability to control of the carrier envelope offset (CEO), which is the absolute phase slip between laser pulses. The mode-locked laser also contains various frequency components in the hundred of terahertz region. These regularly spaced components are called a "frequency comb". By controlling the phase and amplitude of individual comb lines, it would be possible to synthesize an optical field waveform directly like an electric pulse waveform can, which would contribute to the control of laser-matter interactions.

We need a CEO-locked frequency comb with more than a 10-GHz repetition rate in order to resolve each mode of the frequency comb with an arrayed-waveguide grating. The problem is that the pulse energy decreases as the repetition rate increases. We therefore need to achieve CEO locking with a small and high-repetition-rate device with low pulse energy. Recently, we demonstrated a CEO-locked frequency comb with 230-pJ fiber coupling pulse energy [1]. To generate an octave-bandwidth spectrum in a nonlinear fiber and of the second harmonic in an f -to- $2f$ interferometer with low pulse energy, we used a tellurite photonic crystal fiber (PCF) and a periodically poled LiNbO₃ ridge waveguide, respectively. However, we had to use a pulse energy of about 1 nJ because the coupling efficiency of the output of the laser to the PCF. To solve this problem, we propose a method for modifying the optical components in a collinear f -to- $2f$ interferometer. We use angled V-groove splicing between the tellurite PCF and a high-NA fiber to increase coupling efficiency into the tellurite PCF. In addition, we set up the collinear f -to- $2f$ interferometer with the minimum number of optics without an additional dispersion compensation fiber in order to reduce connection and propagation losses. Using our method, we have demonstrated a CEO-locked frequency comb at telecommunications wavelengths with 500-pJ pulse energy, which breaks the previous record of 600 pJ [2] and is, to the best of our knowledge, the lowest pulse energy ever achieved for CEO locking [3]. We believe that our method is useful for lower pulse energy and for long-term stability due to the simple setup.

[1] A. Ishizawa et al., *Opt. Express* **16** (2008) 4706.

[2] I. Hartl et al., *Opt. Express* **13** (2005) 6490.

[3] A. Ishizawa et al., CLEO/IQEC 2009, Baltimore, U.S.A. (May 2009).

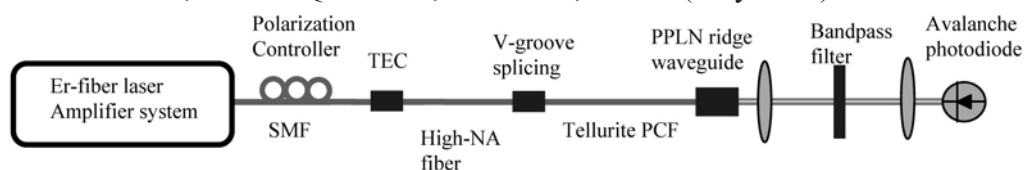


Fig. 1. Experimental setup for the CEO locking with low pulse energy. SMF: single-mode fiber. TEC: thermally expanded core.

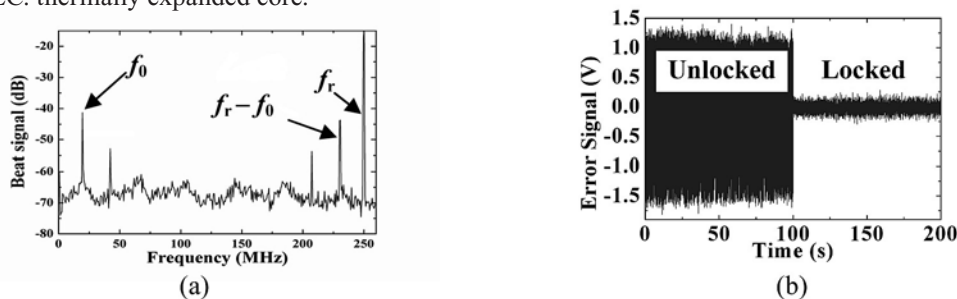


Fig. 2. (a) Self-referencing beat signal of the 250-MHz laser. f_0 : CEO frequency. f_r : repetition rate of the laser. (b) The phase difference between the beat signal and local oscillator.

Cavity Emission and Photon Statistics in Exciton-Cavity Coupled Systems

Takehiko Tawara, Hidehiko Kamada, and Stephen Hughes*
Optical Science Research Laboratory, *Queen's University

Interaction between single exciton and single cavity mode are fundamentally interesting and useful in the context of single-photon source for quantum information processing. A curious feature in recent studies using semiconductor photonic-crystal (PhC) is much brighter cavity emission under large detuning than theoretically expected from standard emission formulas [1]. Here, we undertake an experimental study to identify the cavity mode emission at non-zero detuning and its influence on single photon statistics [2].

We use PhC cavities which consist of a GaAs membrane containing a single InAs dot layer. The left panel of Fig. 1 is image of PL intensity mapping with cavity mode detuning at 4 K. The GaAs barrier was excited by Ar-ion laser (2.54 eV) in this measurement. We found that this system show the bright cavity emission even under fairly-large detunings. The integrated PL intensity when the cavity mode and the exciton are resonant (zero detuning), increases by a factor of about 9 compared with the off resonant case.

To explore the influence of the cavity emission on the photon statistics, we measured the second-order autocorrelation function of the photon intensity. When off-resonant cavity mode, anti-bunching was not observed where $g_C^{(2)}(0) \sim 1$. This absence of the non-classical correlation on the cavity mode is attributed to independently emitted photons from the background such as deep defect level in the GaAs layer. The off-resonant exciton exhibited partial anti-bunching with $g_X^{(2)}(0) = 0.57$, indicating that quantum mechanical coupling prevails. Interestingly, at zero detuning the autocorrelation of the overlapping exciton and cavity modes shows a better anti-bunching with $g_{C+X}^{(2)}(0) = 0.35$. As the exciton-cavity coupling is stronger, the relative weight of the deep states recombination contribution decrease, thereby the anti-bunching behavior is recovered to a better $g^{(2)}(0)$, indicating that the photon statistics becomes more non-classical. These measurements are well explained using a medium-dependent master equation model.

This work was partially supported by Strategic Information and Communications R&D Promotion Programme (SCOPE) of Japan.

[1] For example, K. Hennessy et al., Nature **445** (2007) 896.

[2] T. Tawara et al., Opt. Express **17** (2009) 6643.

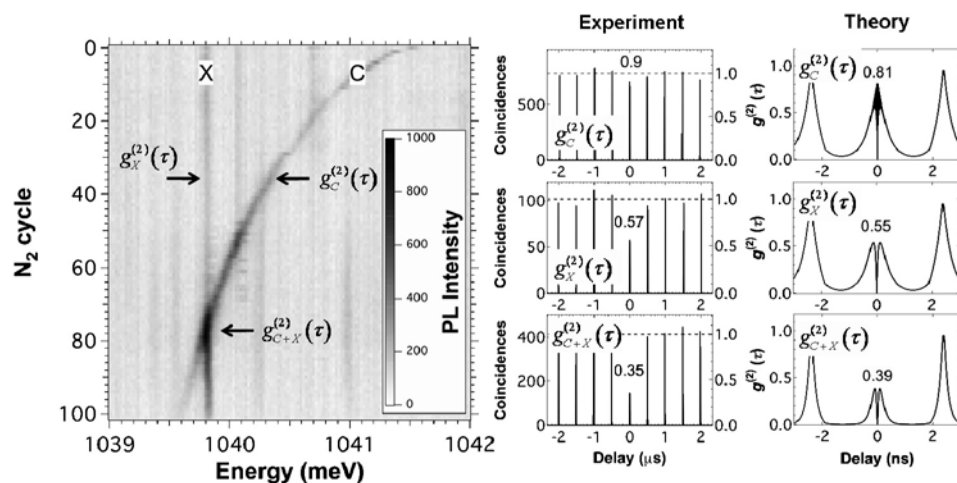


Fig. 1. PL intensity mapping with cavity mode detuning and 2nd order autocorrelation functions.

Magneto-Optical Spectroscopy of Charge-Tunable Quantum Dots

Haruki Sanada, Tetsuomi Sogawa, Hideki Gotoh,
Yasuhiro Tokura, and Hidehiko Kamada
Optical Science Laboratory

Spin states in semiconductor nanostructures are expected to act as quantum information carriers in solid-state systems. One approach that allows us to access single electron spin in semiconductor quantum dots (QDs) is to use negative trions, which serve as an intermediary for the initialization [1] and readout [2] of single electron spins. Most experimental studies have focused on their *lowest* radiative states, however, their *excited* states have a rich variety of configurations because Coulomb and/or exchange interactions between different shells are quite different from those in the lowest shells. In this study, we investigated the magneto-photoluminescence (PL) properties of excited trions in a charge-tunable QD [3].

Our sample consists of monolayer-fluctuation GaAs QDs embedded in an *n-i*-Schottky diode grown by molecular beam epitaxy. For micro-PL measurements, the sample was cooled to 6 K in a cryostat placed in a magnetic field B , which was applied to the sample in the Faraday geometry. A Ti:sapphire laser excited QDs within an aperture in the metal mask/electrode, and the PL spectra were measured with a monochromator and CCD detector.

Figure 1 shows typical PL spectra obtained at $B=0$. Two lines labeled X^0 and X^- are assigned to the lowest-lying neutral exciton and negative trion, respectively. Figure 2 shows a magnetic field dependence of polarization-resolved PL spectra. In addition to X^0 and X^- emissions, we found several PL lines (labeled A~E), most of which exhibit much complex B dependencies. To understand the origin of these PL lines, we consider shell and spin configuration of excited trions. From a configuration-interaction calculation using an elliptic Fock-Darwin model, we obtained the B dependence of trion and electron energies, and found possible assignments of shell and spin configurations for the origin of lines A-E. We believe that the present work opens the possibility of developing a novel scheme for the optical control of single electron spins using the excited states of trions in QDs.

This work was partly supported by KAKENHI (19310067).

- [1] M. Atatüre et al., *Science* **312** (2006) 551.
- [2] D. Press et al., *Nature* **456** (2008) 218.
- [3] H. Sanada et al., *Phys. Rev. B* **79** (2009) 121303.

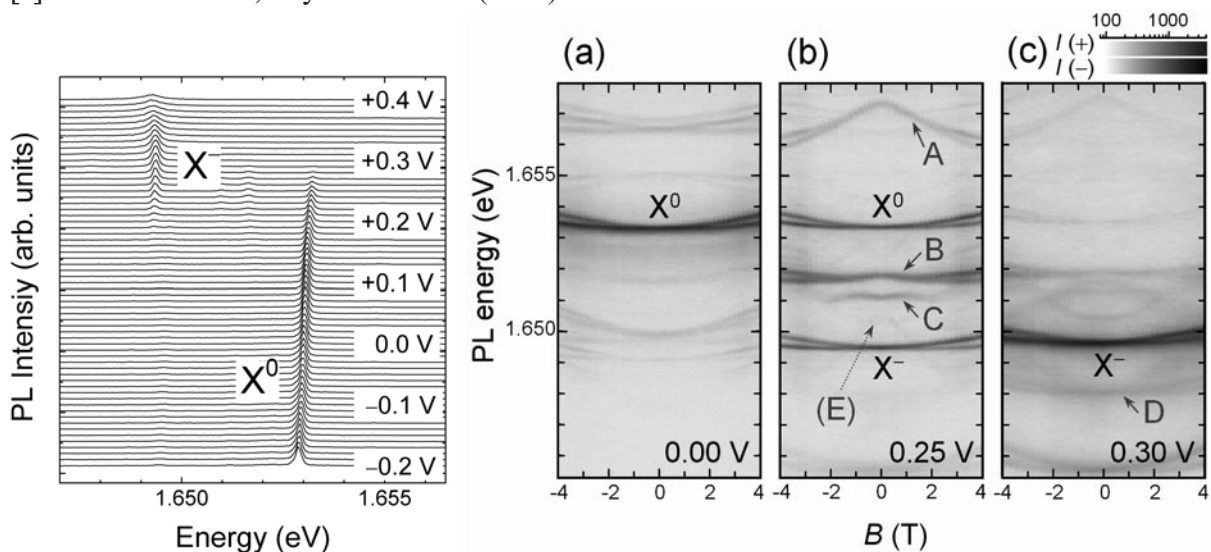


Fig. 1. PL spectra at zero magnetic field.

Fig. 2. Magnetic field evolution of the polarization resolved PL spectra at (a) 0, (b) 0.25 (c) 0.3 V.

Short Pulse Generation by Adiabatic Wavelength Shifting

Takasumi Tanabe, Masaya Notomi, Hideaki Taniyama, and Eiichi Kuramochi
Optical Science Laboratory

Photonic crystal (PhC) nanocavities can trap light for longer than a ns in a volume of less than a μm^3 [1]. We propose a new concept for controlling light that involves manipulating the properties of photons while holding them. This approach has not been previously considered because of the high speed of light. For example, we can change the wavelength of light in the same way as the tone of a vibrating string. The tone of a string can be changed by modulating its tension even after it has been plucked. When the photon lifetime of a cavity is sufficiently long we can change the wavelength of the trapped light by changing the resonance of the cavity [2]. We call this phenomenon *adiabatic wavelength shifting*. Here we describe an adiabatic wavelength shifting experiment and a demonstration of a short pulse released from a high- Q cavity by applying this phenomenon [3]. The demonstration of photon release with arbitrary timing from a high- Q cavity on a chip is the first step toward the development of a true optical memory.

Figure 1 is a scanning electron microscope image of a width-modulated line defect PhC nanocavity [1, 4]. Because the cut-off wavelength of a line defect depends on its width, a cavity is created by shifting the air holes slightly towards the outside of a narrow line defect. Wider line defects are used as i/o waveguides. The cavity is charged with input laser light, and then the input is suddenly turned off to record the behavior of the trapped photons (Fig. 2). We resolved the output wavelengths, and then recorded their waveforms and confirmed that the output decays exponentially without any change in its wavelength when no modulation is applied to the cavity. However, when we apply a pump pulse at a timing of 0 ps from the top of the slab, a short wavelength component appears, which is due to adiabatic wavelength shifting. As a result of the carrier-plasma dispersion effect, both the cavity resonance and the trapped photons shift toward a shorter wavelength.

When the trapped photons shift towards a shorter wavelength, they become closer to the cut-off wavelength of the narrow line defects. As a result, the confinement barriers become shallower and the light in the cavity can couple more strongly with the i/o waveguides. This enables the immediate extraction of the captured light into the waveguides (Fig. 3). We showed that a pulse with a very small width can be obtained by dynamically changing the coupling strength of the trapped light with the i/o waveguides via adiabatic wavelength shifting.

- [1] T. Tanabe et al., *Nature Photon.* **1** (2007) 49.
- [2] M. Notomi et al., *Phys. Rev. A* **73** (2006) 051803.
- [3] T. Tanabe et al., *Phys. Rev. Lett.* **102** (2009) 043907.
- [4] E. Kuramochi et al., *Appl. Phys. Lett.* **93** (2008) 111112.

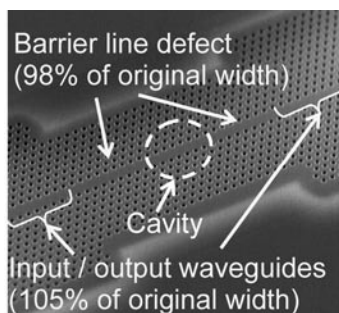


Fig. 1. Width-modulated line defect PhC nanocavity.

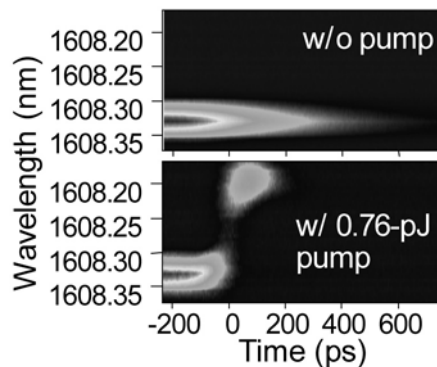


Fig. 2. Spectrogram of the output light. (up) w/o modulation (down) w/ modulation.

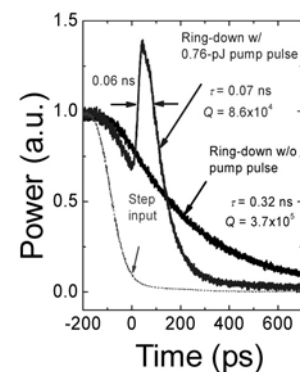


Fig. 3. Output waveform w/ and w/o modulation.

Ultra-high-Q Photonic Crystal Slab Nanocavities in Very Thin Barriers

Eiichi Kuramochi, Hideaki Taniyama, Takasumi Tanabe,
Akihiko Shinya, and Masaya Notomi
Optical Science Laboratory

We have developed width-modulated photonic crystal (PhC) slab line-defect nanocavities with an ultrahigh Q (calculation: $\sim 10^8$, experiment: $\sim 10^6$) [1]. The main advantage of a PhC nanocavity over other micro-cavities is its ultrasmall *mode volume*, which is usually about $0.1 \mu\text{m}^3$ or less. However, conventional PhC nanocavity designs require a thick PhC barrier, which considerably increases the net cavity size. It was believed that a thick photonic bandgap barrier was needed to prevent light leaking from the nanocavity. In this study, we propose a new design scheme that uses a pair of long air slots, which act as low refractive index barriers in the side directions, instead of thick PhC barriers. Here the main role of the thin side PhC is to create a mode-gap barrier in the line defect direction. We demonstrate that the new design scheme preserves most of the performance characteristics of ultrahigh- Q nanocavities [1] even when the PhC slab barriers are very thin [2].

Figure 1 shows suitably designed nanocavities with air slots fabricated in a Si membrane. A width modulated nanocavity is placed exactly at the center of the narrow part. In spite of the very thin side PhC barrier (rows of holes in side PhC: q was 3 and 4), the samples show very high Q values of 5.2×10^5 and 1.3×10^6 , respectively. Figure 2 compares nanocavities with and without air slots as a function of PhC barrier thickness. The highest Q obtained for the thick barrier sample was 1.8×10^6 . Figure 2 clearly demonstrates that the air slots greatly improve the Q value when the side PhC barrier is very thin. Very recently, an advanced design realized an experimental Q of 10^6 at $q=3$ and 3.2×10^5 at $q=2$ [3]. The new cavity design greatly reduces the net size of an ultrahigh- Q PhC nanocavity. Moreover, the new cavity design is very suitable for the study of opto-mechanics because it easily realizes a compact narrow beam with very light weight. A possible application is a mechanical oscillator with built-in high- Q optical nanocavity.

[1] Kuramochi et al., Appl. Phys. Lett. **88** (2006) 041112.

[2] Kuramochi et al., Appl. Phys. Lett. **93** (2008) 111112.

[3] Kuramochi et al., The 8th International Photonic & Electromagnetic Crystal Structures Meeting (PECS-VIII), Sydney, Australia (April 2009).

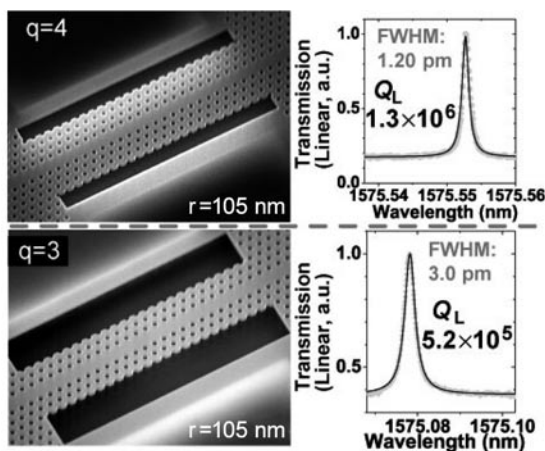


Fig. 1. Electron microscope images and resonant spectra for $q=4$ and $q=3$, respectively.

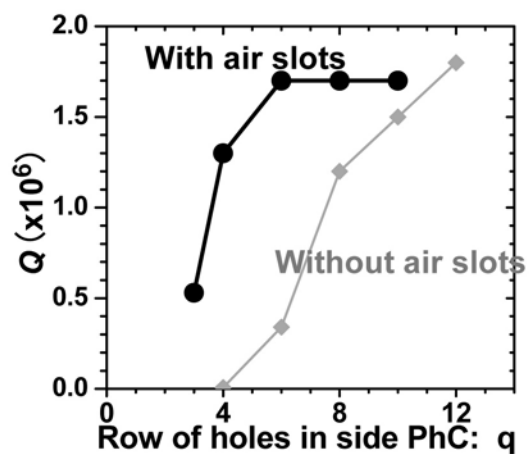


Fig. 2. Experimental Q value of nanocavities in thin PhC barriers (thickness: q rows).

Dynamic High- Q Cavity Formation and Photon Pinning by Index Modulation

Masaya Notomi and Hideaki Taniyama
Optical Science Laboratory

Recently, ultrahigh- Q nanocavities have been realized by small local structural modulation of (typically, several nm shift of the air hole position) line-defect waveguides in two-dimensional photonic crystals [1] [Fig. 1(a)]. This confinement mechanism has been applied to various systems. Periodic structural modulation has realized large-scale ultrahigh- Q coupled nanocavities [2], and ultrahigh- Q nanocavity modes have been also found in one-dimensional systems for the first time by the structural modulation scheme [3].

Here we report that we have found similar ultrahigh- Q cavity modes can be formed only by refractive-index modulation of line-defect waveguides without any structure modulation [4]. The most amazing feature of this finding is that extremely small index modulation can realize ultra-strong light confinement. For example, a Q value higher than 10^7 is possible with index modulation as small as $\Delta n/n=4\times 10^{-4}$. In the case of $\Delta n/n=3\times 10^{-3}$, the calculated Q reaches a surprisingly high value of 5 billions.

Such small index modulation can be achieved by various ultrafast optical nonlinearity. Thus, it may become possible to dynamically form an ultrahigh- Q cavity by local optical pumping. If so, we can pin (in other words, freeze) a part of an optical pulse traveling in a line-defect waveguide by shining a focused light pulse from the top surface. Figure 2 shows a numerical simulation of this process, which indeed shows that the light intensity inside the tuned area marked by a circle is *pinned* in a dynamically-formed cavity mode [4]. Detailed analysis has showed that this process is driven by adiabatic wavelength conversion recently experimentally observed in our group [5].

These results indicate that we can freely control ultrastrong light confinement by very small modulation, which may open up novel functionalities in future optical devices.

- [1] T. Tanabe et al., Nature Photon. **1** (2007) 49.
- [2] M. Notomi, E. Kuramochi et al., Nature Photon. **2** (2008) 741.
- [3] M. Notomi et al., Opt. Express **16** (2008) 11095.
- [4] M. Notomi and H. Taniyama, Opt. Express **16** (2008) 18657.
- [5] T. Tanabe et al., Phys. Rev Lett. **102** (2009) 043907.

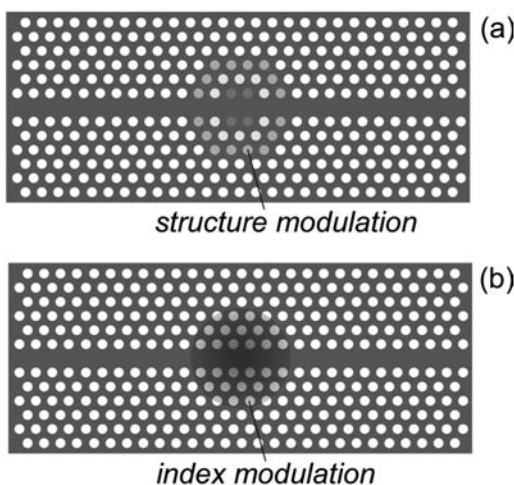


Fig. 1. Ultrahigh- Q cavities formed by local modulation of line-defect waveguide.

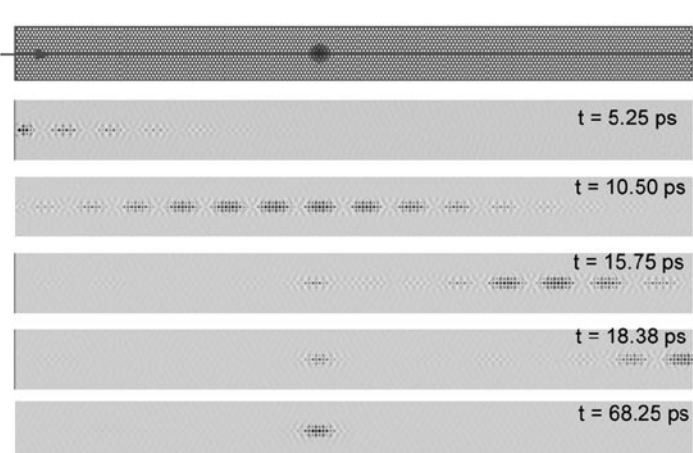


Fig. 2. Numerical simulation of photon pinning induced by dynamic index modulation of a line-defect waveguide.

II . Data

Science Plaza 2008

"Science Plaza 2008", an open-house event at NTT Basic Research Laboratories (BRL), was held at NTT Atsugi R&D Center on Thursday, November 21st, 2008. Under the banner "Nanoscience Opens Up the Quantum World", Science Plaza aimed to present our latest research accomplishments to a wide variety of people both inside and outside NTT and to gather a wide range of opinions.

Following an opening address by Dr. Junji Yumoto, the director of BRL, one of distinguished technical members of NTT BRL, Dr. Masaya Notomi, gave a lecture entitled "Stopping, Caging Light - Manipulation of light by photonic crystals -". In the afternoon session, Prof. Hiroyuki Sakaki, the vice-president of Toyota Technological Institute, gave a special lecture entitled "Quantum Physics of Nano Space and the World of the 21st Century - Think about the ideal way of science and technology in the future -". Each lecture was well attended and followed by stimulating question-and-answer sessions.

Forty-eight poster exhibits, including 16 from Photonics Laboratories and Microsystem Integration Laboratories, presented our latest research accomplishments. These poster exhibits revealed the originality and impact of our research achievements, as well as their future prospects. The posters were intensively discussed, and many thought-provoking opinions were heard. Each year we offer a "Lab Tour", which is a guided tour of the research facilities at NTT BRL that has received high praise from visitors over the years. This year's tour included four different labs, so that as many people as possible could participate. This time we also opened a booth explaining the NTT R&D recruitment system for job-seeking researchers and students. After all the lectures, presentations, and exhibitions had finished, we held a banquet in the center's dining room, where lively conversation among the participants helped to forge personal bonds.

More than 180 people from research institutes, universities, and industry, as well as from NTT Group, attended Science Plaza 2008. Thanks to the efforts of all the participants, the conference ended on a high note. We would like to take this opportunity to express our sincere gratitude to everyone who took part.



International Symposium on Nanoscale Transport and Technology (ISNTT2009)

The International Symposium on Nanoscale Transport and Technology (ISNTT2009) was held from January 20 to 23, 2009, at the NTT Atsugi R&D Center. Since 2000, we have organized two series of international symposia at NTT. One was the International Symposium on Nanoelectronics, Nanostructures, and Carrier Interactions (NNCI) and the other was the Mesoscopic Superconductivity and Spintronics (MS+S). We found that the two symposia had a large overlap in scope in areas such as quantum computation, spintronics, nanoelectronics, or mesoscopic transport. With the aim of further advancing studies in these areas, the idea of jointly organizing these two symposia was then discussed and we finally decided to merge them as a new series, ISNTT, in order to stimulate discussions among researchers in these closely related fields. The symposium was chaired by Dr. Hiroshi Yamaguchi and Dr. Koichi Semba of NTT Basic Research Laboratories, together with Prof. Toshimasa Fujisawa of the Tokyo Institute of Technology. It aspired to gather leading scientists and provide a forum for discussing the most recent topics in the research fields.

In this symposium, we had an excellent opportunity to hear many extremely interesting and very high-quality scientific talks that highlight new aspects and future directions in the research fields of nanoscale transport and technology. There were totally 25 excellent invited talks, including the plenary talk by Prof. Heiblum from Weizmann Institute in Israel, and the special talk by Prof. Leggett from the University of Illinois in the US. Totally 104 contributed oral and poster presentations were given in 17 sessions. The major topics were semiconductor nanodevices, semiconductor micro/nanomechanics, quantum solid state physics, superconducting quantum physics, and semiconductor spintronics. The total number of attendees was 202. We believe that we provided a very nice opportunity for mutual communication within and among the related research fields.



The 5th Advisory Board

The Advisory Board, an external committee whose role is to evaluate the work of NTT Basic Research Laboratories (BRL), met from February 16~18, 2009. This was the fifth meeting of the Advisory Board, which was first convened in 2001 to provide an objective evaluation of our research plans and activities to enable us to employ strategic management in a timely manner. On this occasion, we were happy to welcome a new member.

Over the course of the three days the board made valuable suggestions and comments related to our research and management activities. They agreed that the research level is generally high on an international scale, and that it is important for us to maintain this top-level research and transmit information about our research achievements to the world. They also raised several issues related to human resources, the research budget and internal and external collaboration. We plan to make improvements based on these valuable suggestions.

At this meeting we held a poster session for the first time, and offered researchers an opportunity to communicate with the board members. This included a dinner party for the researchers at which they met and talked with the board members. For the BRL and NTT executives, we organized a Japanese style dinner, which provided a good chance to discuss the future management strategy of NTT BRL from an international perspective. The next board meeting will held in two years.



NTT Basic Research Labs.
Advisory Board Meeting

Walter Schottky, Hans Mooij, Neilson
Boris Altshuler, Massimo, John Ryan
Gerd Klitzing, Junji Yamamoto

February 16-18, 2009

Board Members

Prof. G. Abstreiter

Prof. B. Altshuler

Prof. T. Hänsch

Prof. S. Haroche

Prof. M. Jonson

Prof. T. Leggett

Prof. H. Mooij

Prof. J. Ryan

Prof. K. von Klitzing

Affiliation

Walter Schottky

Columbia Univ.

Max-Planck-Inst.

École Normale

Chalmers Univ. of Tech.

Univ. of Illinois

Delft Univ. of Tech.

Univ. of Oxford

Max-Planck-Inst.

Research Field

Low-dim. Semiconductor Physics

Condensed Matter Physics

Quantum Optics

Quantum Optics

Condensed Matter Physics

Quantum Physics

Quantum Physics

Nano-bio Technology

Semiconductor Physics

Award Winners' List (Fiscal 2008)

ITU-T Kaleidoscope Academic Conference: Innovations in NGN - Future Network and Services Best Paper Award, Second Place	H. Takesue T. Honjo K. Tamaki Y. Tokura	Differential Phase Shift Quantum Key Distribution	May 13, 2008
The 52nd International Conference on Electron, Ion, and Photon Beam Technology and Nanofabrication (EIPBN-2008) Micrograph Contest Best Video Award	K. Yamazaki H. Yamaguchi	The Mini-faces of Egypt	May 28, 2008
The Laser Society of Japan The 32st Original Paper Award	K. Oguri Y. Okano T. Nishikawa H. Nakano	Spatiotemporally Dynamics Study of a Femtosecond Laser Ablation Plume Based on Ultrafast XAFS Spectroscopy	May 30, 2008
JJAP Award for the Best Original Paper	K. Suzuki K. Kanisawa S. Perraud M. Ueki K. Takashina Y. Hirayama	Imaging of Interference Between Incident and Reflected Electron Waves at an InAs/GaSb Heterointerface by Low-temperature Scanning Tunneling Spectroscopy	Sep. 2, 2008
The Japan Society of Applied Physics Young Scientist Award for the Presentation of Excellent Paper	H. Okamoto	Q -control and Self-oscillation of GaAs Cantilevers by Carrier Excitation	Sep. 2, 2008
The 141st Committee on Microbeam Analysis of Japan Society for the Promotion of Science (JSPS) Sakaki Encouragement Award	H. Hibino	Dynamical Observations of Crystal Growth and Phase Transition by Surface Electron Microscopy	Sep. 16, 2008
JSPS Prize	M. Notomi	Discovery and Applications of Novel Functions of Photonic Crystals	Mar. 9, 2009
Japan Academy Medal	M. Notomi	Discovery and Applications of Novel Functions of Photonic Crystals	Mar. 9, 2009

In-house Award Winners' List (Fiscal 2008)

Idea Contest 2008 Highest Award for Service Idea	M. Yamaguchi K. Uchiyama T. Hashimoto	Time-capsule Service on Denwa-channel	Nov. 11, 2008
Bronze Award for NGN Application	N. Taniguchi K. Shimizu		
NTT R&D Award	T. Honjo H. Takesui K. Inoue	Differential Phase Shift Quantum Cryptography	Dec. 18, 2008
NTT R&D Award	I. Mahboob	Development of Electromechanical Devices for Logic Processing Utilizing Tiny Mechanical Vibration	Dec. 18, 2008
Award for Achievements by Director of Basic Research Laboratories	A. Shinya T. Tanabe E. Kuramochi H. Taniyama M. Notomi S. Matsuo T. Kakitsuka T. Sato	Development of All-optical Bit Memory by Photonic Crystals	Mar. 19, 2009
Award for Achievements by Director of Basic Research Laboratories	Y. Ono M. Khalafalla	Development of Single-dopant Technology	Mar. 19, 2009
Award for Excellent Papers by Director of Basic Research Laboratories	I. Mahboob	"Bit Storage and Bit Flip Operations in an Electromechanical Oscillator", Nature Nanotechnol. 3 (2008) 275.	Mar. 19, 2009
Award for Excellent Papers by Director of Basic Research Laboratories	K. Nishiguchi	"Stochastic Data Processing Circuit Based on Single Electrons Using Nanoscale Field-effect Transistors", Appl. Phys. Lett. 92 (2008) 062105.	Mar. 19, 2009
Award for Excellent Papers by Director of Basic Research Laboratories	H. Nakashima	"Self-Assembly of Gold Nanorods Induced by Intermolecular Interactions of Surface-Anchored Lipids", Langmuir 24 (2008) 5654.	Mar. 19, 2009
Special Award by Director of Basic Research Laboratories	K. Oguri T. Tawara H. Sumikura H. Okamoto H. Shibata	Contribution to the Rearrangement of the Laboratory Equipments	Mar. 19, 2009
Special Award by Director of Basic Research Laboratories	A. Tokura Y. Kobayashi	Health Risk Management of Carbon Nanotubes	Mar. 19, 2009

List of Visitors' Talks (Fiscal 2008)

I. Materials Science

Date	Speaker	Affiliation "Title"
May. 23	Prof. Erhard Kohn	University of Ulm, Germany "Recent Progress in Diamond Related Device Work at Ulm"
Sep. 29	Prof. Satoru Tanaka	Kyushu University "Formation of Heterostructures by SiC Surface Nano-Facets and Surface Self-Reformation"
Sep. 29	Mr. Kenjiro Hayashi	Kyushu University "Analysis of Stacking Sequence of Graphene Layers Formed on SiC Surface"
Oct. 7	Prof. Jonathan Heddle	Tokyo Institute of Technology "Bionanoengineering with Protein Rings"
Oct. 14	Prof. Seigi Mizuno	Kyushu University "Analysis of Surface Structure by Low-Energy Electron Diffraction and Development of Nano Area Probes"
Dec. 12 Dec. 19 Dec. 26	Prof. Jocelyn Achard	Université Paris 13, France "Fundamentals of Diamond CVD Growth Process"
Mar. 24	Mr. Yoshihiko Kuroki	Sony Corporation "Improvements in Motion Image Quality by High Frame Rate"

II. Physical Science

Date	Speaker	Affiliation "Title"
Apr. 15	Dr. Nicolas Clément	University of Sciences and Technologies of Lille, France "Toward Electrical Detection of Single Molecules: Description of the Project and Presentation of Dynamic Electrical Transport and Noise in Molecular Junctions"
Jun. 9	Dr. Norikazu Mizuochi	University of Tsukuba "Generation and Retrieval of Entangled States from Single Spins in Diamond at Room Temperature"
Jun. 23	Dr. Simon J. Devitt	University of Cambridge, U.K. University of Melbourne, Australia "Subspace Confinement: How Good Is Your Qubit?"
Jul. 2	Dr. Ryosuke Ishiguro	Tokyo University of Science "Supersolid vs. Superfluid at Grain Boundaries"
Jul. 3	Prof. Seth Lloyd	Massachusetts Institute of Technology, U.S.A. "Quantizing the Global Positioning System" "Quantum Computation and Photosynthesis"
Jul. 29	Prof. Cun-Zheng Ning	Arizona State University, U.S.A. "Semiconductor Nanolasers: Is There an End to Miniaturization?"
Nov. 25	Prof. Yasuhiro Hatsugai	University of Tsukuba "Universality of the Zero Gap Semiconductors: From Graphene and d-wave Superconductors to Topological Insulators"
Dec. 4	Dr. Samuel Deléglise	École Normale Supérieure, France "Generation and Time-resolved Reconstruction of Cavity Field Quantum States"

Dec. 17	Prof. Saverio Pascazio	University of Bari, Italy "Antibunching and Correlations of Field-Emitted Electrons from a Superconductor"
Jan. 19	Prof. Jörg Schmiedmayer	Technische Universität Wien, Austria "Atom Chips"
Feb. 23	Prof. Wilfred G. van der Wiel	University of Twente, the Netherlands "Hybrid Organic-inorganic Systems for (Spin) Electronics"
Feb. 26	Prof. Klaus H. Ploog	Paul-Drude-Institut, Germany "Challenges in Materials Science for Sustainable Energy"
Mar. 2	Mr. Nobuyuki Kambe, CTO	NanoGram Corporation, U.S.A. "Global Nanotech Venture: Publick Contribution through Innovative Technologies"

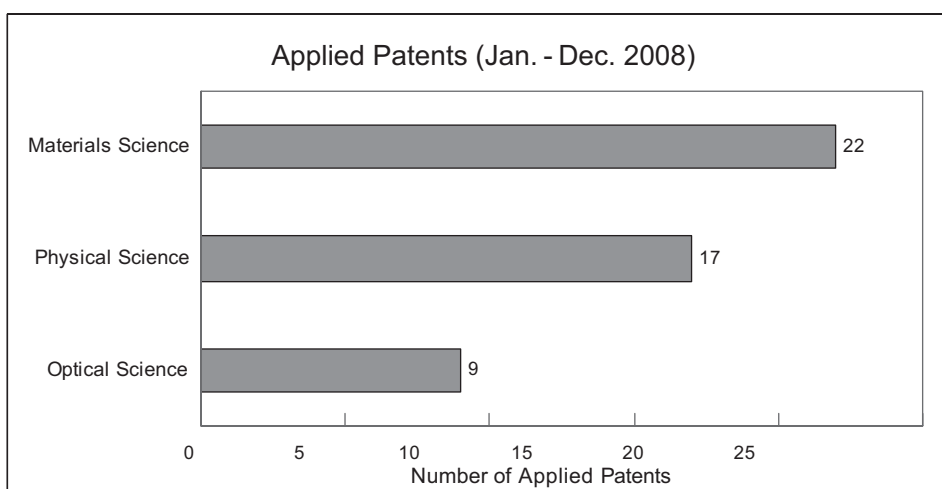
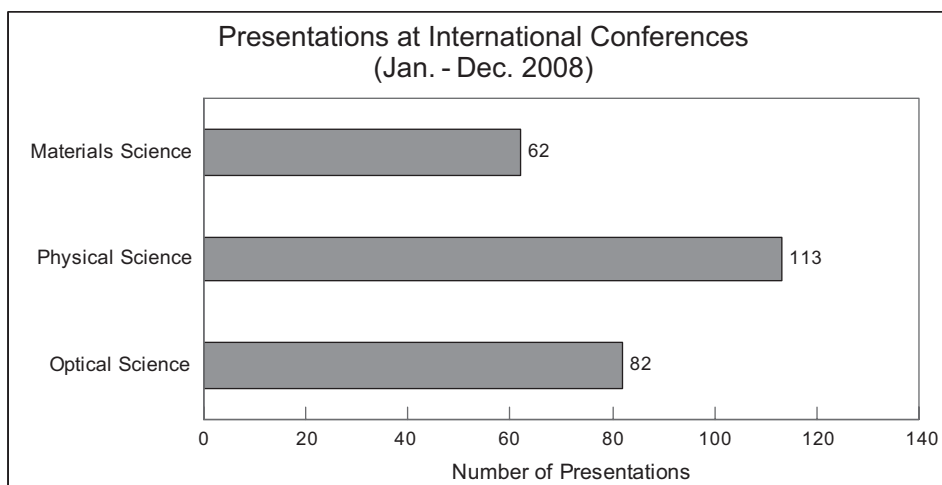
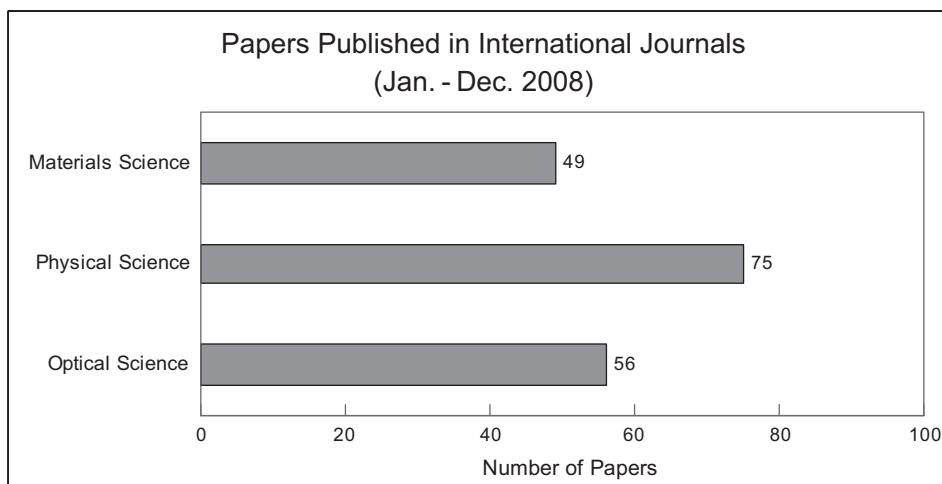
III. Optical Science

Date	Speaker	Affiliation "Title"
Aug. 11	Prof. Tsuneyuki Ozaki	University of Quebec, Canada "Unique High-order Harmonic Generation from Plasma at the Advanced Laser Light Source"
Oct. 9	Prof. Stephen Hughes	Queen's University, Canada "Unraveling the Light-matter Interactions of "Disorder-induced Scattering" and the "Strong-coupling Regime" in Semiconductor Nanostructures"
Oct. 10	Prof. Amnon Aharony	Ben-Gurion University of the Negev, Israel "Spin Filtering by a Periodic Spintronic Device"

Oct. 15	Prof. Ora Entin-Wohlman	Ben-Gurion University of the Negev, Israel "The Conductance of Superconducting-normal Hybrid Structures"
Oct. 23	Prof. Yong-Hee Lee	Korea Advanced Institute of Science and Technology, Korea "Spatial and Spectral Nano-control of Micro-resonators"
Nov. 18	Prof. Christos Flytzanis	Ecole Normale Supérieure, France "Coherent Optically Driven Electron Charge/Spin Transport and Magnetic Ordering in Polar Photonic and Magnetophotonic Structures"
Dec. 2	Dr. Yasumitsu Miyata	National Institute of Advanced Industrial Science and Technology "Optical properties of metallic and semiconducting single-wall carbon nanotubes"
Dec. 22	Dr. Tetsuya Ido	National Institute of Information and Communications Technology "Pulse Amplification of Optical Frequency Combs by Using a Passive Optical Cavity and $^1S_0-^3P_1$ Transition of Sr in Optical Lattice Clock"
Jan. 7	Mr. Akira Ozawa	Max-Planck-Institut, Germany "Towards Precision Spectroscopy with XUV Frequency Comb"

Research Activities in Basic Research Laboratories in 2008

The numbers of papers published in international journals, presentations at international conferences and applied patents in year 2008 amounted to 180, 257, and 48, respectively. The numbers for each research area are as follows;



The numbers of research papers published in the major journals are shown below.

Journals	(IF2007*)	Numbers
Advanced Materials	8.191	1
Applied Physics Express	-	3
Applied Physics Lettters	3.596	16
Applied Surface Science	1.406	6
Diamond and Related Materials	1.788	7
Japanese Journal of Applied Physics	1.247	19
Journal of Applied Physics	2.171	4
Langmuir	4.009	2
Nano Letters	9.627	3
Nanotechnology	3.31	3
Nature Nanotechnology	14.917	1
Nature Photonics	-	1
Nature Physics	14.677	5
Optics Express	3.709	12
Physica E-Low-Dimensional Systems & Nanostructures	0.834	19
Physical Review A	2.893	3
Physical Review B	3.172	16
Physical Review Letters	6.944	10

*IF2007: Impact Factor 2007 (Journal Citation Reports,2007)

The average IF2007 for all research papers from NTT Basic Research laboratories is 3.07.

The numbers of presentations in the major conferences are shown below.

Conferences	Numbers
The Conference on Lasers and Electro-Optics and the Quantum Electronics and Laser Science Conference	13
The IEEE Nanotechnology Materials and Device Conference 2008	10
International Symposium on Physics of Quantum Technology	10
International Symposium on Surface Science and Nanotechnology	10
The International Conference on the Physics of Semiconductors	9
25th International Conference on Low Temperature Physics	8
2008 International Conference on Solid State Devices and Materials	7
21st International Microprocesses and Nanotechnology Conference	6
The 9th International Symposium on Foundations of Quantum Mechanics in the Light of New Technology	6
13th Advanced Heterostructures and Nanostructures Workshop	4
The American Physical Society	4
18th International Conference on High Magnetic Fields in Semiconductor Physics and Nanotechnology	4
Mechanical Systems in the Quantum Regime, the Gordon Research Conferences	4
The 5th International Conference on Physics and Applications of Spin-related Phenomena in Semiconductors	4
The International Symposium on Graphene Devices: Technology, Physics, and Modeling	4
The 23rd Nishinomiya-Yukawa Memorial International Workshop	4
The 21st Annual Meeting of The IEEE Lasers & Electro-Optics Society	4
The 9th International Conference on Quantum Communication, Measurement and Computing	4
International Symposium on Growth of III-Nitrides	4

List of Invited Talks at International Conferences (2008)

I. Materials Science Laboratory

- (1) H. Hibino, "Microscopic determination of number of graphene layers on SiC", Symposium on Surface and Nano Science 2008, Appi, Japan (Jan. 2008).
- (2) S. Suzuki and Y. Kobayashi, "Low-energy irradiation damage in single-walled carbon nanotubes: defect characteristics and electric property control", International Carbon Nanotube Conference in Nagoya University, Nagoya, Japan (Feb. 2008).
- (3) K. Torimitsu, Y. Shinozaki, and Y. Furukawa, "Magnesium effect on brain neural development", Gordon Research Conferences, Magnesium in biochemical processes and medicine, Ventura, USA, (Mar. 2008).
- (4) K. Torimitsu, Y. Shinozaki, and Y. Furukawa, "Magnesium effect on rat brain neural development in vitro", European Magnesium Meeting 2008, Paris, France, (May 2008).
- (5) Y. Taniyasu and M. Kasu, "Influence of dislocation on AlN deep-UV light-emitting diodes", 4th Asian Conference on Crystal Growth and Technology, Sendai, Japan (May 2008).
- (6) Y. Kobayashi, T. Akasaka, and T. Makimoto, "Boron Nitride Grown by MOVPE", 14th International Conference of Metalorganic Vapor Phase Epitaxy, Metz, France (June 2008).
- (7) K. Torimitsu, "Development of Nanobio Interface using Neurons and Receptor Proteins", Asia-Pacific Symposium on Nanobionics, Wollongong, Australia (June 2008).
- (8) A. Shimada, N. Kasai, and K. Torimitsu, "Conductive-Polymer Microelectrode Array for Neural Signal Measurements", 16th Annual International Conference on Composites/Nano Engineering, Kuming, China (July 2008).
- (9) H. Hibino, "Number-of-layers dependence of electronic properties of epitaxial graphene investigated by SPELEEM", 5th International Workshop on Nanoscale Spectroscopy and Nanotechnology, Athens, U.S.A. (July 2008).
- (10) H. Omi, D. P. Sprunken, K. Furukawa, H. Nakashima, I. Sychugov, Y. Kobayashi, and K. Torimitsu, "Determination of Aspect Ratio Distribution of Gold Nanorods from Absorption Spectra using Gans Theory", 16th Annual International Conference on Composites/Nano Engineering, Kuming, China (July 2008).
- (11) Y. Taniyasu and M. Kasu, "MOVPE Growth of Single-crystal Hexagonal AlN on Cubic Diamond", 2nd International Symposium on Growth of III-Nitride, Izu, Japan (July 2008).
- (12) M. Kasu, K. Ueda, H. Kageshima, and Y. Taniyasu "Challenges of Diamond-based Electronic Devices", International Conference on Electronic Materials 2008, Sydney, Australia (July 2008).
- (13) K. Torimitsu, Y. Shinozaki, A. Shimada, and Y. Furukawa, "Receptor based nano-bio research: application to medical bionics", Sir Mark Oliphant International Frontiers of Science and Technology Conference Series, Inaugural Conference on Medical Bionics, Lorne, Australia (Nov. 2008).
- (14) K. Torimitsu, "Receptor protein functions and its application for biomimetic device", The 5th Sweden-Japan Workshop on Bio-Nanotechnology, Stockholm, Sweden (Nov. 2008).
- (15) H. Hibino, H. Kageshima, M. Kotsugi, and Y. Watanabe, "Local work function measurements of epitaxial few-layer grapheme", 5th International Symposium on Surface Science and Nanotechnology, Tokyo, Japan (Nov. 2008).

- (16) K. Torimitsu, "Protein-based nanobio research for medical bionics", 8th International Symposium on Advanced Fluid Information and Transdisciplinary Fluid Integration, Sendai, Japan (Dec. 2008).

II. Physical Science Laboratory

- (1) Y. Ono, "Single boron detection in nano-scale SOI MOSFETs", The 2009 International Meeting for Future of Electron Devices, Kansai, Osaka, Japan (May 2008).
- (2) K. Kanisawa, "Imaging surface states bound to native donors at the epitaxial InAs surface", Nanoscale Spectroscopy & Nanotechnology 5 - Spin-Polarized Scanning Tunneling Microscopy 2, Athens, U.S.A. (July 2008).
- (3) A. Fujiwara and Y. Ono, "Single-Electron Device", ITRS (International Technology Roadmap for Semiconductors) - ERD (Emerging Research Devices) Workshop on Maturity Evaluation for Selected Beyond CMOS Emerging Technologies, San Francisco, U.S.A. (July 2008).
- (4) I. Mahboob and H. Yamaguchi, "The quantum Hall effect probed via a parametrically pumped electromechanical resonator", Frontiers of Low Temperature Physics, London, U.K. (Aug. 2008).
- (5) H. Yamaguchi and I. Mahboob, "Micro/Nanomechanical Systems for Information Processing", The 9th International Symposium on Foundations of Quantum Mechanics in the Light of New Technology, Saitama, Japan (Aug. 2008).
- (6) H. Yamaguchi, I. Mahboob, H. Okamoto, and K. Onomitsu, "Micro/Nanomechanical Systems Based on Semiconductor Heterostructures", The International Symposium on Compound Semiconductors, Rust, Germany (Sep. 2008).
- (7) Y. Ono, M. A. H. Khalafalla, A. Fujiwara, K. Nishiguchi, K. Takashina, S. Horiguchi, Y. Takahashi, and H. Inokawa, "Single-dopant effect in Si MOSFETs", IEEE Nanotechnology Materials and Device Conference, Kyoto, Japan (Oct. 2008).
- (8) K. Semba, "Cavity-QED with Quantum Superconducting Circuits", Quantum information, quantum coherence and related topics, Tokyo, Japan (Sep. 2008).
- (9) H. Nakano, S. Saito, K. Semba, and H. Takayanagi, "Quantum Analysis on Superconducting Qubit Readout with a Josephson Bifurcation Amplifier", Quantum Dynamics in Dots and Junctions: Coherent Solid State Systems, Riva del Garda, Italy (Oct. 2008).
- (10) K. Grove-Rasmussen, H. I. Jorgensen, T. Hayashi, P. E. Lindelof, and T. Fujisawa, "Electronic transport in carbon nanotube quantum dots", Korea Conference on Innovative Science and Technology, Phoenix Park, Korea (Oct. 2008).
- (11) H. Yamaguchi, "Novel Functionalities in Semiconductor-based Micro/Nanomechanical Systems", 21st International Microprocesses and Nanotechnology Conference, Fukuoka, Japan (Oct. 2008).
- (12) I. Mahboob and H. Yamaguchi, "Bit operation in a parametrically pumped electromechanical resonator", Nano Technology 2008, Ishikawa, Japan (Oct. 2008).
- (13) A. Fujiwara, K. Nishiguchi, Y. Ono, H. Inokawa, and Y. Takahashi "Silicon Single-Electron Devices and Their Applications", TND 2008 Technical Forum, Seoul, Korea (Oct. 2008).
- (14) T. Ota, T. Hayashi, and T. Fujisawa, "Quantum information processing devices with nano-scale semiconductor quantum dots", 1st Russian-Japanese Young Scientists Conference on Nanomaterials and Nanotechnology, Moscow, Russia (Oct. 2008).

- (15) K. Semba, "Quantum control of the flux qubit coupled to microwave photon system", Solid State Quantum Information, Pisa, Italy (Dec. 2008).
- (16) K. Grove-Rasmussen, "Quantum Transport in Carbon Nanotubes", Workshop on novel phenomena at nanoscale interface, Hsinchu, Taiwan (Dec. 2008).

III. Optical Science Laboratory

- (1) H. Takesue, "Quantum communication experiments using entangled photons generated in dispersion shifted fiber", LEOS Winter Topical Meeting of Nonlinear Photonics, Sorrento, Italy (Jan. 2008).
- (2) M. Notomi, T. Tanabe, E. Kuramochi, A. Shinya, and H. Taniyama, "Nonlinear and adiabatic control of light in a photonic crystal chip", LEOS Winter Topical Meeting of Nonlinear Photonics, Sorrento, Italy (Jan. 2008).
- (3) T. Tanabe, E. Kuramochi, A. Shinya, H. Taniyama, and M. Notomi, "Photonic crystal nanocavities with extremely long photon lifetime and their applications", The 6th Asia Pacific Laser Symposium, Nagoya, Japan (Jan. 2008).
- (4) S. Kawanishi, M. Tanaka, M. Ohmori, and H. Sakaki, "Photonic bandgap fiber for new wavelength range", Optical Fiber Communication Conference and Exposition/National Fiber Optics Engineers Conference, San Diego, U.S.A. (Feb. 2008).
- (5) M. Notomi, "Control of Light by Photonic Crystal Nanocavities", JST-DFG Workshop on Nanoelectronics, Aachen, Germany (March 2008).
- (6) M. Yamashita and M.W. Jack, "Number squeezing of an array of Bose-Einstein condensates trapped in a 1D optical lattice", 17th International Laser Physics Workshop, Trondheim, Norway (June 2008).
- (7) T. Honjo, S. W. Nam, H. Takesue, Q. Zhang, H. Kamada, Y. Nishida, O. Tadanaga, M. Asobe, B. Baek, R. Hadfield, S. Miki, M. Fujiwara, M. Sasaki, Z. Wang, K. Inoue, and Y. Yamamoto, "Entanglement-based BBM92 QKD experiment using superconducting single photon detectors", 17th International Laser Physics Workshop, Trondheim, Norway (June 2008).
- (8) T. Tanabe, A. Shinya, E. Kuramochi, and M. Notomi, "Nonlinear Switching in High-Q Photonic Crystal Nanocavities", Integrated Photonics and Nanophotonics Research and Applications, Boston, U.S.A. (July 2008).
- (9) S. Kawanishi, "Recent Progress in Photonic Crystal Fiber Technologies", Opto-Electronics and Communications Conference, Sydney, Australia (July 2008).
- (10) M. Notomi, T. Tanabe, E. Kuramochi, and H. Taniyama, "Slow Light Media Based on Ultrahigh-Q Nanocavities", OSA Topical Meeting on Slow and Fast Light, Boston, U.S.A. (July 2008).
- (11) H. Takesue, H. Fukuda, T. Tsuchizawa, T. Watanabe, K. Yamada, Y. Tokura, and S. I. Itabashi, "Entanglement generation using silicon wire waveguide", 5th International Conference on Group IV Photonics, Sorrento, Italy (Sep. 2008).
- (12) H. Takesue, K. Harada, H. Fukuda, T. Tsuchizawa, T. Watanabe, K. Yamada, Y. Tokura, and S. I. Itabashi, "Entanglement generation using silicon wire waveguide", International Conference on Quantum Optics and Quantum Information, Vilnius, Lithuania (Sep. 2008).
- (13) H. Nakano, A. Ishizawa, and K. Oguri, "Dependence of surface harmonics generation properties on carrier-envelope phase of few-cycle laser field", Advanced coherent light sources, Hilo, U.S.A. (Sep. 2008).

- (14) H. Takesue, H. Fukuda, T. Tsuchizawa, T. Watanabe, K. Yamada, Y. Tokura, and S. I. Itabashi, "Entangled photon-pair generation using silicon photonic wire waveguide", The IEEE Nanotechnology Materials and Device Conference, Kyoto, Japan (Oct. 2008).
- (15) M. Notomi, A. Shinya, T. Tanabe, E. Kuramochi, H. Taniyama, S. Matsuo, T. Kakitsuka, and T. Sato, "On-chip All-optical Processing Based on Photonic Crystal Nanocavities", Asia Optical Fiber Communication & Optoelectronic Exposition and Conference, Shanghai, China (Oct. 2008).
- (16) S. Kawanishi, "Recent Progress in Photonic Bandgap Fiber Technology", Asia Pacific Optical Communications, Hangzhou, China (Oct. 2008).
- (17) Y. Tokura, "Quantum spin transport in magnetic-field-engineered nano-structures", Spin Transport in Condensed Matter, The 23rd Nishinomiya-Yukawa Memorial International Workshop, Kyoto, Japan (Oct. 2008).
- (18) H. Takesue and T. Honjo, "Quantum communication experiments using telecom-band entangled photons", The 21st Annual Meeting of The IEEE Lasers & Electro-Optics Society, Newport Beach, U.S.A. (Nov. 2008).
- (19) K. Oguri, Y. Okano, T. Nishikawa, and H. Nakano, "Dynamic imaging of femtosecond laser ablation plume by using laser-generated soft x-ray", The 21st Annual Meeting of The IEEE Lasers & Electro-Optics Society, Newport Beach, U.S.A. (Nov. 2008).
- (20) H. Nakano, A. Ishizawa, and K. Oguri, "Interference between surface harmonics of carrier-envelope phase controlled few-cycle laser field", International Society for Photo-optical Instrumentation Engineers, Wuahn, China (Nov. 2008).
- (21) K. Tamaki, "Unconditional security proof of QKD and imperfections of devises", Updating Quantum Cryptography 2008, Tokyo, Japan (Dec. 2008).
- (22) Y. Tokura, "Latest progress in QKD experiments at NTT", Updating Quantum Cryptography, Tokyo, Japan (Dec. 2008).

**Research Activities in NTT-BRL
Editorial Committee**

NTT Basic Research Laboratories

3-1 Morinosato Wakamiya, Atsugi

Kanagawa, 243-0198 Japan

URL: <http://www.brl.ntt.co.jp/>